A human relevant mixture of persistent organic pollutants induces reactive oxygen species formation in isolated human leucocytes: Involvement of the β2-adrenergic receptor

Hanne Friis Berntsen [a,b,*], Johanna Bodin [c], Johan Øvrevik [d,e], Christopher Friis Berntsen [f,g], Gunn C. Østby [a], Bendik C. Brinchmann [b,d], Erik Ropstad [a], Oddvar Myhre [d]

[a] Department of Production Animal Clinical Sciences, Faculty of Veterinary Medicine, Norwegian University of Life Sciences, P.O. Box 5003 NMBU, NO-1432 Ås, Norway
[b] National Institute of Occupational Health, P.O. Box 5330, Majorstuen, 0304 Oslo, Norway
[c] Department of Methods Development and Analytics, Norwegian Institute of Public Health, N-0456 Oslo, Norway
[d] Department of Environmental Health, Norwegian Institute of Public Health, N-0456 Oslo, Norway
[e] Department of Biosciences, University of Oslo, Norway
[f] Department of Internal Medicine, Sykehuset Innlandet Hospital Trust, Gjøvik, Norway
[g] Department of Internal Medicine, Lovisenberg Diaconal Hospital, Oslo, Norway

ARTICLE INFO

ABSTRACT

Exposure to chlorinated (Cl), brominated (Br) and perfluoroalkyl acid (PFAA) persistent organic pollutants (POPs) is associated with immunotoxicity and other adverse effects in humans and animals. Previous studies on POPs have mainly focused on single chemicals, while studies on complex mixtures are limited. Using DCF and luminol assays we examined effects on ROS generation in isolated human neutrophils, monocytes and lymphocytes, after in vitro exposure to a total mixture and sub-mixtures of 29 persistent compounds (Cl, Br, and PFAA). The mixtures were based on compounds prominent in blood, breast milk, and/or food. All mixture combinations induced ROS production in one or several of the cell models, and in some cases even at concentrations corresponding to human blood levels (compound range 1 pM – 16 nM). Whilst some interactions were detected (assessed using a mixed linear model), halogenated subgroups mainly acted additively. Mechanistic studies in neutrophils at 500× human levels (0.5 nM – 8 μM) indicated similar mechanisms of action for the Cl, PFAA, the combined PFAA + Cl and total (PFAA + Br + Cl) mixtures, and ROS responses appeared to involve β2-adrenergic receptor (β2AR) and Ca^{2+} signalling, as well as activation of NADPH oxidases. In line with this, the total mixture also increased cyclic AMP at levels comparable with the non-selective βAR agonist, isoproterenol. Although the detailed mechanisms involved in these responses remain to be elucidated, our data show that POP mixtures at concentrations found in human blood, may trigger stress responses in circulating immune cells. Mixtures of POPs, further seemed to interfere with adrenergic pathways, indicating a novel role of βARs in POP-induced effects.

1. Introduction

Persistent organic pollutants (POPs) are resistant to degradation, are widely distributed throughout the environment, and may bioaccumulate in living organisms and biomagnify through the food chain (Secretariat of the Stockholm Convention, 2019). Whereas the highly lipophilic chlorinated and brominated POPs accumulate mainly in lipid rich tissues such as adipose tissue and blood lipids, the perfluorinated compounds bind to proteins including plasma proteins, and are found in relatively high concentrations in blood as compared to other POPs

---

(range calculated average: 0,28–16.4 nM for the Scandinavian population, Supplementary Table S1) (Jones et al., 2003; Karrman et al., 2006; Lau and Luch, 2012). POPs may thus potentially affect circulatory immune cells, however, documentation of the impact of realistic POP mixtures on immune cells remains scarce. In a recently published systematic review, (Martin et al., 2020) reported immunotoxicological studies to be largely underrepresented among mixture studies conducted over the last 10 years.

Previous studies in humans and animals report adverse effects of POPs from all three halogenated groups on immune parameters. Chlorinated compounds such as polychlorinated biphenyls (PCBs) have been reported to affect immunoglobulin concentrations in humans (Nakanishi et al., 1985; Heilmann et al., 2006) and suppress B-cell mediated immunity in salmons (Arkoosh et al., 1994). Moreover, experimental data suggest that also organochlorine pesticides may affect human immune function, although available epidemiological studies were unable to establish immunotoxic risk associated with pesticide exposure (Corsini et al., 2013). The polybrominated diphenyl ether (PBDE) congener BDE-209, at concentrations similar to levels found in occupationally exposed workers, has been reported to adversely affect the number and functionality of immune cells in mice (Zeng et al., 2014). In line with this the sum of PBDEs was also reported to be negatively associated with lymphocyte numbers in an epidemiological study (Leijs et al., 2009). Increased levels of perfluoroalkyl substances have been associated with a reduced response to vaccination in both animal studies as well as in humans (Grandjean et al., 2012; Grandjean et al., 2017; Grandjean et al., 2017; Abraham et al., 2020; EFSA, 2020). This effect was recently considered by the European Food Safety Authorities (EFSA, 2020) to be the current most critical factor for establishment of a tolerable weekly intake for perfluoroalkyl substances in food.

The innate immune system is the first line of defence against invading microorganisms. Immune cells such as neutrophils, monocytes and macrophages destruct phagocytosed microorganisms through so-called respiratory burst: production of high levels of reactive oxygen species (ROS), predominately superoxide, within the phagosome by membrane bound NADPH oxidase (Selvatici et al., 2006). As such, NADPH oxidase plays a central defence function against pathogens, and a deficiency of this system may lead to immunosuppression. However, excess or sustained ROS production cause cellular stress, and is considered a central factor in the development of a range of chronic and immunological disorders (Panday et al., 2015). In contrast to the phagocytic cells, lymphocytes, which participate in both innate (NK cells) and adaptive (T and B cells) immunity, produce ROS mainly through lipid metabolism, in mitochondria or via activation of NADPH oxidase (Jackson et al., 2004). Previous studies have shown that exposure to selected PCBs or PBDEs may induce ROS formation in human neutrophils (Voie et al., 1998; Voie et al., 2000; Reistad and Mariussen, 2005; Myhre et al., 2009; Berntsen et al., 2016). Increased ROS production was also observed in isolated human lymphocytes exposed to perfluorooctanesulfonic acid (PFOS) (Zarei et al., 2018), and ROS formation, as well as alterations in antioxidant levels, have been reported in splenocytes and thymocytes from mice after 7 days oral exposure to PFOS (Zhang et al., 2013).

In the current study, the probes $2'$-$7'$dichlorofluorescin diacetate (DCFH-DA) and luminol were used to measure cellular formation of ROS. DCFH-DA is cell-permeable and hydrolyses intracellularly to the DCFH carboxylate anion, which is retained within the cell. Oxidation of DCFH by ROS results in the formation of the fluorescent dichlorofluorescein (DCF), which can be detected by techniques like fluorimetry. DCFH is useful for ROS detection as it can potentially be oxidised by several different reactive species formed by cells, including peroxynitrite, hydrogen peroxide (when a catalyst is present, such as a heme, a peroxidase, or cytochrome c) and hydroxyl radicals, providing an overall index of oxidative stress. On the other hand, it is not suitable for detection of e.g. nitric oxide, hypochlorite or superoxide in biological systems (Myhre et al., 2003; Wrona and Wardman, 2006; Karlsson et al.,

2010). Experiments also show that peroxide-dependent DCF fluorescence is dependent on intracellular glutathione levels (Tampo et al., 2003), catalase, hydroxyl radical scavengers and iron chelating agents (LeBel et al., 1992). There are several limitations related to the use of this probe. As an example, DCF may produce superoxide and hydrogen peroxide via reaction of DCF radical with oxygen, thus increasing the ROS formation that it is attempting to quantify. Also, transition metals (including redox-active iron), cytochrome c, and heme peroxidases can catalyse DCFH oxidation (LeBel et al., 1992; Kalyanaraman et al., 2012). As a result of these limitations the use of a combination of several ROS detection techniques is usually recommended. Luminol is also frequently used in studies of ROS production in leucocytes. Luminol is sensitive towards HOCl formation (Myhre et al., 2003), and it shows increased luminescence in the presence of hydrogen peroxide when combined with sodium hypochlorite, in addition to e.g. free metal ions, biological complexes between metal ions and organic components and enzymes belonging to oxidoreductases (e.g. respiratory complexes I, II and III in mitochondria) (Khan et al., 2014). Luminol has the advantage that it detects both intra- and extra-cellular ROS as it can diffuse into cells (Jancinová et al., 2006).

Catecholamines such as adrenaline and noradrenaline are among the central regulators of immune function, immune cells, and brain-immune cross talk, acting through adrenoceptors (ARs) expressed on immune cells (Scanzano and Cosentino, 2015). The role of adrenergic pathways in regulating innate immunity has gained attention, and it is now clear that βARs may suppress neutrophil migration, CD11/CD18 expression and oxidative metabolism (Scanzano and Cosentino, 2015). Canonically, the βARs couple to Gs proteins activating adenylyl cyclases (AC) which results in increased intracellular cyclic adenosine monophosphate (cAMP) (Seifert and Schultz, 1991). However, βARs can also couple to Gi and Gq proteins in addition to β-arrestin, resulting in different responses from those activated through Gs proteins (Wenzel-Seifert et al., 1991; Audet and Bouvier, 2008; Drake et al., 2008; Rosenbaum et al., 2009; Evans et al., 2010). βARs may also initiate redox signalling via membrane-bound NADPH oxidase. While transient activation of βARs elicits modest increases in ROS, prolonged activation has been reported to induce high ROS levels in glial cells (Rambacher and Moniri, 2020). Of particular interest, it has become clear that polycyclic aromatic hydrocarbons (PAHs) may interact directly with β2AR, and PAH-mixtures have been shown to impair β2AR function (Factor et al., 2011; Chu et al., 2013). Moreover, benzo[a]pyrene (BaP) was reported to bind with high affinity to the ligand binding pocket of β2ARs, and trigger cAMP and calcium signalling in human embryonic kidney cells, leading to subsequent β2AR-desensitisation by receptor endocytosis (Mayati et al., 2012; Mayati et al., 2017). The toxicological implications of interactions between PAHs and β2ARs remain unclear, but the potential of pollutants interfering with adrenergic pathways is concerning, given the central role of adrenoceptors in immune regulation as well as lung and cardiovascular disease (Bernstein et al., 2011; Scanzano and Cosentino, 2015; Le Ferrec and Øvrevik, 2018). However, whether POPs may also affect β2ARs remains to be determined.

Most studies examining effects of POPs on the immune system use single compounds, and often at high concentrations. However, as we are exposed simultaneously to a large number of chemicals in real life, it is important to study mixtures at environmentally relevant concentrations. When chemicals cooccur, they may act additively, displaying non-interaction effects, which is currently believed to be the most common scenario, especially at low concentrations (Kortenkamp et al., 2009; Martin et al., 2020). They may also in certain situations, although less commonly observed, display interactive synergistic (more than additive) or antagonistic (less than additive) effects. Such deviations from additivity must be investigated using an additivity model such as dose addition, independent action or a mixed model (Kortenkamp et al., 2009; Martin et al., 2020). It has also been observed that chemicals acting through a similar (in comparison to dissimilar) mode of action targeting the same signalling pathway may more potently compromise

cellular defence and recovery mechanisms (Ermler et al., 2013; Pistollato et al., 2020).

We have previously designed two different mixtures of 29 POPs comprising the same chlorinated, brominated and perfluorinated compounds for use in *in vitro* (named total mixture), and *in vivo* studies (not used in the present study, for details see Berntsen et al. (2017)) based on a literature review on levels of POPs from the Scandinavian population (Berntsen et al., 2017). As we constructed two mixtures, one for incorporation into feed for *in vivo* studies, and one for use in *in vitro* studies, we selected representative compounds that were prominent in either blood, breast milk or food from the following chemical groups: chlorinated compounds (organochlorine pesticides and polychlorinated biphenyls), brominated compounds and perfluorinated compounds. As such the design was thus not focused on a specific mode of action. The *in vitro* mixture containing all the 29 POPs (total mixture) was based on average levels of POPs in blood from the Scandinavian population. To allow for the study of effects attributed to a specific halogenated group, or interactive effects between groups, we also constructed six sub-mixtures containing only one or combinations of two chemical group (s), for further details see Berntsen et al. (2017) and Materials and methods Section 2.2. Using these mixtures, we have previously reported a reduction in the phagocytic capacity of isolated and monocyte-derived macrophages, however after use of relatively high concentrations (4000× human blood levels), which was partly associated with cytotoxicity (Berntsen et al., 2018). Here, we explore the effects of lower, non-cytotoxic concentrations of these mixtures (1–500×) on production of ROS in human leucocytes, with emphasis on the potential role of NADPH oxidases and β2AR signalling.

2. Materials and methods

2.1. Chemicals and reagents

The chlorinated compounds and PBDE congeners used for the mixtures were purchased from Chiron AS (Trondheim, Norway). The perfluorinated compounds (with the exception of tridecafluorohexane-1-sulfonic acid potassium salt (PFHxS)), hexabromocyclododecane (HBCD), 5-amino-2,3-dihydro-1,4-phtalazindione (luminol; ≥97%), carvedilol, dextran from Leuconostoc spp (Mr 450,000–650,000), dimethyl sulfoxide Hybri-Max™ (DMSO; ≥99.7%), diphenyleneiodonium chloride (DPI), (−)-isoproterenol hydrochloride (≥98 %), ICI 118,551 hydrochloride (ICI; ≥98%), methanol (MeOH; ≥99.9 %), 2-methyl-2H-pyrazole-3-carboxylic acid (2-methyl-4-o-tolylazo-phenyl)-amide (CH-223191, ≥98%), Percoll® (cell culture tested), propranolol and salmeterol xinafoate (≥98%) were supplied by Sigma-Aldrich (St. Louis, MO, USA). PFHxS (>98%) was from Santa Cruz Biotechnology, Inc, Santa Cruz, CA, USA. Lymphoprep™ was obtained from Axis-Shield (Oslo, Norway). 1,2-bis(o-aminophenoxy)-ethane-N,N,N'N'-tetraacetic acid tetraacetoxymethyl ester (BAPTA-AM) was obtained from Calbiochem (San Diego, CA, USA). 2',7'- dichlorodihydrofluorescein diacetate (DCFH-DA), Hanks' Balanced Salt Solution (HBSS; 10×) and HEPES buffer, came from GIBCO/Invitrogen (Oslo, Norway). Stock solutions of BAPTA-AM, betanaphthoflavone, CH-223191, carvedilol, DPI, propranolol, salmeterol and luminol were all prepared by dissolution in DMSO and frozen and thawed before each experiment (with the exception of luminol which was batched out into small vials for use in each experiment), whereas ICI and isoproterenol were dissolved in sterile water, batched into small vials, thawed before each experiment, and diluted into relevant concentrations in supplemented HBSS. DCFH-DA was dissolved in methanol. All other reagents used were analytical grade laboratory chemicals from standard commercial suppliers.

The Hyperosmotic Percoll was made by mixing of 4.85 ml Percoll with 4.15 ml autoclaved Milli-Q(MQ)-water and 1 ml of 1.6 M NaCl, whereas the Isosmotic Percoll was composed of 4.15 ml Percoll, 4.85 ml MQ-water, and 1 ml 1.5 M NaCl.

2.2. Mixtures of POPs

The mixtures of POPs used in the present study were based on a literature review on the most recent Scandinavian studies published prior to 2012 reporting levels of POPs in blood, breast milk and food. The compounds occurring at the highest levels were selected and incorporated into the mixtures, and chemical concentrations were based on average concentrations in Scandinavian human blood. A mean value was calculated from several studies for each compound where these were available (Berntsen et al., 2017). For the exact values and articles included see Table S2, S5 and S8 of the supplementary material section in Berntsen et al. (2017). In the few cases where no blood values were found; these were extrapolated from values in breast milk. The stocks used in the present study had a concentration of 1000000× times blood levels and were diluted down to relevant concentrations for use in the experiments. 7 different mixtures were used; the perfluoroalkyl acid (PFAA) mixture containing PFHxS, perfluorooctanesulfonic acid potassium salt (PFOS), perfluorooctanoic acid (PFOA), perfluorononanoic acid (PFNA), perfluorodecanoic acid (PFDA) and perfluoroundecanoic acid (PFUnDA), the Br mixture containing polybrominated diphenyl ethers: BDE-47, -99, -100, -153, -154 and -209 as well as HBCD, the Cl mixture containing PCB 28, 52, 101, 118, 138, 153 and 180, *p,p'*-dichlorodiphenyldichloroethylene (DDE), hexachlorobenzene (HCB), α-chlordane, oxychlordane, *trans*-nonachlor, α-hexachlorocyclohexane (HCH), β-HCH, γ-HCH (lindane) and dieldrin, the Br + Cl mixture containing brominated and chlorinated compounds, the PFAA + Cl mixture containing perfluorinated and chlorinated compounds, the PFAA + Br mixture containing perfluorinated and brominated compounds, and the total mixture (PFAA + Br + Cl) containing all three chemical groups (see Table 1). For construction of the 7 mixtures, all compounds were dissolved in appropriate volatile solvent, and the correct amounts of compounds were added to the respective stock solution vials, followed by evaporation of solvents under N_2-flow. The mixtures of dry powder were ultimately dissolved in DMSO. Concentrations of single compounds in the 7 mixtures were kept constant at the same dilutions across the various mixtures, and concentrations in the stocks were measured and verified as described in Berntsen et al. (2017) to ensure that they did not deviate significantly from nominal concentrations. Although some downward deviation from nominal concentrations were found; especially for the perfluorinated group, values were still within the reported range of human values. Representative measured stock concentrations, used for the various mixture combinations in the present study are presented in Table 1. 1× concentrations corresponding to human blood levels are found in Supplementary Table S1. Except for the perfluorinated compounds PFHxS, PFNA, PFDA and PFUnDA, most of the compounds included in the mixtures are defined as POPs under the Stockholm Convention on Persistent Organic Pollutants. Whereas PFHxS is currently proposed for listing under the Stockholm Convention (Secretariat of the Stockholm Convention, 2019), PFNA, PFDA and PFUnDA have also been found to have long elimination half-lives in humans (Freberg et al., 2010; Nilsson et al., 2010). Cells were exposed to one or several concentrations of the mixtures at 1, 10, 100 and 500 or 1000× average human blood levels. Corresponding concentrations of the various chemicals in nM and ng/ml are presented in Supplementary Table S1.

2.3. Isolation of human blood cells:

For the isolation of human blood cells 100 ml of peripheral blood was collected into EDTA-containing tubes (10.8 mg) (BD Vacutainer K2E, BD Biosciences, Franklin Lakes, NJ, USA) from male human voluntaries 30–60 years of age. All participants signed an informed consent, and the experiment was approved by the Regional Committees for Medical and Health Research Ethics (REC 2014/1475), Norway. For use in the experiments the three following cell fractions were isolated: neutrophils, lymphocytes and monocytes.

Table 1

Composition of stock-concentrations in μM at 1000000x human blood levels of the seven different mixtures of persistent organic pollutants (POPs) used for exposure of isolated human leucocytes. These stocks were diluted down, and cells were in the different experiments exposed to one or several concentrations of POPs at 1, 10, 100, 500 or 1000× the average concentration in human blood as calculated in Berntsen et al. (2017).

Mixture	Cl	Br	PFAA	Cl + Br	Cl + PFAA	Br + PFAA	Total mixture
Chlorinated compounds							
PCB 28	31			31	31		31
PCB 52	22			22	22		22
PCB 101	26			26	26		26
PCB 118	131			131	131		131
PCB 138	449			449	449		449
PCB 153	729			729	729		729
PCB 180	378			378	378		378
p,p'-DDE	1089			1089	1089		1089
HCB	235			235	235		235
α - chlordane	30			30	30		30
oxy - chlordane	33			33	33		33
trans-nonachlor	99			99	99		99
α-HCH	18			18	18		18
β-HCH	76			76	76		76
γ-HCH (Lindane)	19			19	19		19
Dieldrin	62			62	62		62
Brominated compounds							
BDE-47		14		14		14	14
BDE-99		6		6		6	6
BDE-100		4		4		4	4
BDE-153		1		1		1	1
BDE-154		2		2		2	2
BDE-209		9		9		9	9
HBCD		65		65		65	65
Perfluorinated compounds							
PFHxS			6910		6910	6910	6910
PFOS			16,370		16,370	16,370	16,370
PFOA			6690		6690	6690	6690
PFNA			1740		1740	1740	1740
PFDA			660		660	660	660
PFUnDA			280		280	280	280

2.3.1. Isolation of human neutrophils

Isolation of human neutrophils for measurements of ROS was carried out by dextran sedimentation and density gradient centrifugation, as described by Boyum et al. (1991). In brief EDTA blood was mixed with 6 % dextran and left for 30 min at room temperature (RT) for the sedimentation of erythrocytes. The supernatant containing neutrophils was subjected to Lymphoprep^{TM} density gradient centrifugation at 625g for 15 min at RT. The resulting layer of mononuclear cells, formed at the interface between supernatant and separation fluid, was removed for further separation of monocytes and lymphocytes, leaving a pellet of neutrophils and erythrocytes at the bottom of the tubes. The pellets were re-suspended in 0.83 % NH$_4$Cl and left for 7 min at RT for lysis of remaining erythrocytes. The tubes were thereafter centrifuged for 7 min at 625g, the supernatant removed, and cells washed twice in 0.9 % NaCl. The resulting pellets were re-suspended in HBSS buffer supplemented with 4.17 mM NaHCO$_3$, 20 mM HEPES and 5 mM glucose. Subsequently, cell number was counted, and cells diluted in supplemented HBSS to a concentration of 2.5×10^6 cells/ml buffer.

2.3.2. Isolation and separation of human monocytes from platelets and dead cells

The mononuclear cells removed during the isolation of neutrophils described above, were further isolated and separated into monocytes and lymphocytes based on the protocol described by Repnik et al. (2003). In brief mononuclear cells were washed with RPMI 1640 medium (from now RPMI) by centrifugation at 350g for 7 min. Washing was repeated once, and cells were re-suspended in RPMI and counted before another centrifugation at 350g for 7 min and removal of the supernatant. Subsequently, the cell pellet was re-suspended in RPMI medium to a concentration of 50–70 × 10^6 cells/ml. 3 ml cells/tube were thereafter layered on top of 10 ml hyperosmotic Percoll and centrifuged

at 580g for 15 min. The monocyte fraction forming at the interface after centrifugation, was removed and washed in RPMI medium by centrifugation at 350g for 7 min. Subsequently, to separate monocytes from dead cells and platelets, the cell pellet was re-suspended in 3 ml RPMI, layered on top of 10 ml isosmotic Percoll, and centrifuged at 350g for 15 min. The resulting pellet was re-suspended in a small amount of RPMI, transferred to a new tube, and washed in RPMI at 350g for 7 min. The pellet was finally re-suspended in 5 ml RPMI and diluted in supplemented HBSS to a concentration of 1.0×10^6 cells/ml buffer.

2.3.3. Isolation of human lymphocytes

The remaining cell pellet from isolation of the monocyte fraction, on the hyperosmotic Percoll described above, was re-suspended in 4 ml overlying medium, and transferred to a new tube, before washing in RPMI at 350g for 7 min. The resulting pellet was re-suspended in 3 ml fresh RPMI, cells counted, and diluted in supplemented HBSS to a concentration of 2.5×10^6 cells/ml buffer.

2.4. Exposure of cells and assessment of ROS-production

ROS production was measured in neutrophils with two different assays, the luminol and the DCF assays. Since the luminol assay had higher sensitivity for ROS detection in the present study, as well as in previous studies (Aam and Fonnum, 2006; Myhre et al., 2009; Berntsen et al., 2016), this assay was chosen for further mechanistic studies performed in neutrophils as well as the measurements of ROS production in lymphocytes and monocytes. Neutrophils, the primary mediators of the rapid innate host defence against most bacterial and fungal pathogens (Malech et al., 2014), were chosen as the cell type for mechanistic studies. The large number of neutrophils obtained during each isolation, as compared to lymphocytes and monocytes, facilitated multiple

analysis. To rule out autoluminescence from chemicals in the mixture causing false positive results, 500× of the total mixture was tested in several wells in one experiment, and no significant deviation from the blank could be observed. Autofluorescence was ruled out in a previous mixture study in a different cell type (primary rat cerebellar granule neurons) using the DCF assay, where no significant ROS production or increase in fluorescence was observed at concentrations up to 4000× human blood levels using the same mixtures (Berntsen et al., 2021). Blank wells containing buffer (neutrophils), or buffer/medium (monocytes and lymphocytes) only were included on all plates and used for subtraction of background noise.

2.4.1. Exposure of neutrophils, lymphocytes and monocytes, and detection of ROS using the luminol assay

Detection of ROS formation in neutrophils, lymphocytes and monocytes with the luminol assay was performed as described by Voie et al. (1998) for neutrophils with minor modifications. Chemiluminescence (from now luminescence) in the presence of luminol, which penetrates the cell membrane, is dependent on the myeloperoxidase-H_2O_2 -Cl^- system and reacts with hypochlorous acid (HOCl) and other ROS, producing detectable luminescence (Dahlgren and Karlsson, 1999; Myhre et al., 2003). For the concentration–response/mechanistic studies, the seven mixtures/mixture and pharmacological compound combinations were added in triplicate to white 96 well-plates (Nunclon) in 50 μl buffer, followed by 100 μl luminol (0.25 mM) and 100 μl cells (2.5×10^6 cells/ml for the neutrophils and lymphocytes, and 1.0×10^6 cells/ml for the monocytes). This resulted in the concentration–response studies in exposures of 1.0×10^6 cells/ml for neutrophils/lymphocytes (n = cells from 6 and 8 different persons, respectively), and 4.0×10^5 cells/ml for monocytes (n = cells from 6 different persons) to concentrations corresponding to 1, 10, 100 and 500× average human blood levels. Luminescence readings were started immediately after addition of cells and were performed repeatedly for 1 h in a CLARIOstar® microplate reader (BMG Labtech, Ortenberg, BW, Germany), with a new reading cycle started approximately every 8.5 min. The AUC was calculated as an expression of cumulative ROS production. For lymphocytes and monocytes, the slopes of the curves were still linear after 1 h. For neutrophils ROS production peaked between 30 and 60 min depending on experiment. For consistency the area under the curve (AUC) after 1 h was used for all cell types.

2.4.2. Exposure of neutrophils and detection of ROS using the DCF-assay

The assessment of ROS production with the DCF assay was carried out mainly as described by Myhre et al. (2000). The DCF-assay is based on the diffusion of the non-ionic probe DCFH-DA across the cell membrane; and its hydrolysis to the non-fluorescent DCFH inside the cell through the action of intracellular esterases. DCFH is oxidised to the fluorescent DCF amongst other when ROS such as $ONOO^-$, $^\bullet OH$ and hydrogen peroxide (H_2O_2) are present. Cells were pre-incubated (4 ml of cells/tube at a concentration of 2.5×10^6 cells/ml buffer) with DCFH-DA (2 μM) for 15 min at 37 °C under light protection, followed by centrifugation at 625g, and re-suspension of the cell pellet in 4 ml of supplemented HBSS buffer without DCFH-DA. The 7 mixtures were added in triplicate to black 96-well plates (Nunclon) in 150 μl buffer, followed by addition of 100 μl of cells (2.5×10^6 cells/ml), resulting in exposure of 1.0×10^6 cells/ml (n = cells from 4 different persons) to concentrations corresponding to 1, 10, 100 and 1000× average human blood levels (from now referred to as 1, 10, 100 and 1000×). DCF fluorescence measurements were started immediately after addition of neutrophils to the plate, and readings performed every minute for 1 h in a VICTOR3 1420 multilabel plate reader (PerkinElmer, Inc. Waltham, MA, USA) at 37℃, with excitation/emission wavelengths of 485/530 nm, and the AUC calculated as an expression of cumulative ROS production.

2.4.3. Mechanistic studies in neutrophils

For the mechanistic studies (n = cells from 4 to 6 different persons), neutrophils were exposed to 500× human blood levels of the total mixture and various concentrations of the following pharmacological compounds: 10, 50 and 100 μM of the selective β2AR antagonist ICI-118551; 1 and 10 μM of the non-selective, competitive β2 antagonists propranolol and carvedilol; 0.1, 1, and 10 μM and 0.5, 1 and 10 μM of the β2 agonists salmeterol and isoproterenol, respectively. Also, the effects of 5 μM of the intracellular calcium chelator BAPTA-AM and 0.1 and 1 μM of the NADPH-oxidase inhibitor DPI were analysed. Further, 1 μM of the aryl hydrocarbon receptor (AhR) antagonist CH-223191 and 1 and 5 μM of the AhR agonist betanaphthoflavone were used. 500× was the highest mixture concentration applied in the luminol assay, which also induced the highest increase in ROS production for most of the mixtures. It was therefore chosen as the mixture concentration for the mechanistic studies to optimise the chances of observing a detectable effect with the pharmacological modulators applied. To determine if similar mechanisms were involved after exposure to the PFAA, the Cl and the PFAA + Cl mixtures, the mechanistic studies were repeated in separate experiments using 500× of these mixtures or the total mixture and 10 and 50 μM ICI, 10 μM carvedilol, 0.1 μM DPI, and 5 μM BAPTA-AM. As negligible ROS production was observed after exposure to the Br-mixture, the Br-containing mixtures were not chosen for further mechanistic studies.

2.5. Cyclic AMP (cAMP) assay:

To further assess the involvement of the β2AR in the mixture-induced ROS production, levels of cAMP were measured using the cAMP-Glo™ Assay kit (Promega, WI, USA) according to the manufacturer's guidelines. In short, neutrophils were incubated in black 96-well plates (Nunclon) with 0.1 % DMSO, 500× of the total mixture, or 1 μM of the β2AR agonist isoproterenol as a positive control for 15 and 30 min. Cells were then lysed with cAMP-Glo™ Lysis Buffer and incubated for 20 min with cAMP Detection Solution containing Protein Kinase A at RT, before incubation with Kinase-Glo® Reagent for another 10 min at RT. Luminescence was then measured in a CLARIOstar® microplate reader (BMG Labtech, Ortenberg, BW, Germany), and cAMP concentrations estimated from a cAMP standard curve (0–4.0 μM cAMP).

2.6. Assessment of cytotoxicity using the LDH-assay

The lactate dehydrogenase (LDH) assay (Biovision, Milpitas, CA, US) was used to determine membrane leakage as a measure of cell death in supernatant from neutrophils exposed for 2 h to 100 and 500× human blood levels of the Cl, PFAA, PFAA + Cl and total mixtures (n = cells from 4 to 6 different persons). 10 μl of the cell supernatants were mixed with 90 μl of the LDH reaction solution and incubated for 30 min. Absorbance was read at 490 nm using a plate reader (EL808 Biotek, Winooski, Vermont, US). Cell death was calculated relative to unexposed DMSO control. LDH assay was only performed with neutrophils due to the limited number of cells received from the other cell fractions.

2.7. Statistical methods:

We fit three linear mixed models for concentration–response experiments using the luminol assay, one for each cell type, all using the area under the curve at one h for luminescence values as the dependent variable. To account for inter-individual differences and intra-individual correlations between observations, we included a random intercept for person. As explanatory variables, we included the presence or absence of each mixture (PFAA, Cl and Br), mixture concentration and whether the observation was a buffer control. Dichotomous explanatory variables were coded as 0 for absence and 1 for presence. DMSO was present at the same concentration in all solutions except buffer, and the model reduces to the estimated cumulative luminescence for the DMSO group when

explanatory variables are all zero or absent. We also included two-way interactions terms between mixtures and between each mixture and concentration.

We selected the most parsimonious model providing the best fit as assessed using Akaike's information criterion (AIC). Additionally, we inspected quantile–quantile plots and residual plots to check whether models gravely violated normality assumptions. We applied a logarithmic transformation to the outcome variable to reduce heteroscedasticity. Starting with a maximalist model, we performed stepwise model reduction by removing interactions and variables with non-significant coefficients. However, we kept all terms also forming part of any interaction included in the final model, and all interactions between mixtures and mixture concentration.

The final models were similar for all cell types. The formula for the linear mixed models is given in Eq. (1):

$$\ln Lumin_{ij} = \beta_0 + \beta_1 PFAA_{ij} + \beta_2 Cl_{ij} + \beta_3 Br_{ij} + \beta_4 Conc_{ij} + \beta_5 PFAA_{ij}Cl_{ij} + \beta_6 PFAA_{ij} \cdot Br_{ij} + \beta_7 Cl_{ij} \cdot Br_{ij} + \beta_8 PFAA_{ij} \cdot Conc_{ij} + \beta_9 Br_{ij} \cdot Conc_{ij} + \beta_{10} Cl_{ij} \cdot Conc_{ij}$$
$$+ \beta_{11} Ctrl_{ij} + b_{0i} + \varepsilon_{ij}$$

$$b_0 \sim N\left(0, \sigma_{b_0}^2\right), \ \varepsilon_{ij} \sim N\left(0, \sigma^2\right) \tag{1}$$

where i denotes the index of the person, j the index of the within-person replication, β_0 the fixed intercept, and b_{0i} the random intercept per person. *PFAA*, *Cl*, and *Br* are categorical variables denoting the presence or absence of each substance; *Ctrl* whether the observation is a control. *Conc* denotes mixture concentration, and *Lumin* the resulting cumulative luminescence. ε_{ij} denotes the error term. ε_{ij} and b_0 were both assumed to be normally distributed.

For the DCF assay experiments, there were too few persons to fit a mixed-effects model. To obtain estimates of overall mean effects, we hence fitted a generalised estimating equation (GEE) using an independence covariance structure. Since model fit is not estimable for GEEs, we specified the equation using the same independent variables as in the final linear mixed models, assuming these would have reasonable explanatory value also for the DCF assay. We applied a Huber-White sandwich estimator to safeguard against misspecification of the covariance structure (Froot, 1989; Williams, 2000).

Both for the mixed models and the GEE, we computed predicted mean outcome values for linear combinations of explanatory variables corresponding to the mixture and concentration combinations investigated, as well as the DMSO control. To determine whether each exposed group was significantly different from DMSO, we applied a Dunnett's post-hoc test. Significance levels were adjusted for multiple comparisons using a Bonferroni-Holm correction. We likewise assessed whether a concentration–response relationship was present for each mixture using a Dunnett's post-hoc test, determining whether linear combinations of coefficients containing concentration terms applicable to each mixture were significantly different from zero.

To estimate effects of pharmacological compounds on ROS production in neutrophils exposed to different combinations of mixtures, we fit a mixed-effects model using a grouping factor denoting exposure to mixture, pharmacological compound and pharmacological compound concentration as the explanatory variable. We included a random intercept for person with the same rationale as above. Comparisons of interest between estimated reductions in luminescence for mixture combinations with or without pharmacological compounds were likewise done with a Dunnett's test with Bonferroni-Holm correction, using relevant combinations without pharmacological compounds as control. To illustrate the magnitude of the effect of pharmacological compounds,

we computed the corresponding relative reduction in luminescence compared to mean values for mixture combinations without pharmacological compounds. The values were expressed as % reduction ±95% CI.

We did all mixed-model and GEE analyses and plotting in R (R Core Team, 2019), using the packages lme4 (Bates et al., 2014), lmerTest (Kuznetsova et al., 2017), geepack (Yan, 2002; Yan and Fine, 2004; Halekoh et al., 2006), multcomp (Hothorn et al., 2008), broom (Robinson et al., 2019), dplyr (Wickham and François, 2019), data.table (Dowle and Srinivasan, 2019) and ggplot2 (Wickham, 2016). R syntax for the final models is provided in Supplementary material S2.

For cAMP measurements, fold change values were calculated and expressed relative to the values in the DMSO control, and significant differences assessed using a two-way ANOVA with a Holm-Sidak's multiple comparisons test.

Cell death after chemical exposure was calculated relative to response from DMSO exposed cells in the LDH-assay, expressed as % increase in LDH compared to DMSO control, and significant differences from control were assessed using a one-way ANOVA.

In all the experiments conducted, a p-value of < 0.05 was regarded as statistically significant.

3. Results

3.1. ROS production assessed using luminol-amplified chemiluminescence

3.1.1. Human neutrophils

The model for luminescence induced in neutrophils measured with the luminol assay indicates a clear positive concentration–response relationship for the PFAA and Cl mixtures (both, $p < 0.001$), but not for Br ($p = 0.30$). There was a small, but significant positive interaction between the Br and Cl mixtures ($p < 0.05$), indicating a minimal synergistic effect of these compounds in mixtures where both were present (Br + Cl mixture and total mixture). Table 2 shows the model coefficients in bold, where values greater than 1 for interaction terms indicate synergism and values below 1 antagonism. Concentration-response coefficients are displayed in Table 3.

Fig. 1 shows results from *post-hoc* hypothesis testing for comparisons between each tested mixture combination and DMSO control, as well as the estimated concentration–response curves for each combination. The Cl mixture induced significantly more luminescence at $100\times$ ($p < 0.05$) and $500\times$ ($p < 2 \times 10^{-16}$) blood concentration. The Br + Cl combination was only significantly different from DMSO at $500\times$ blood concentration ($p < 2 \times 10^{-16}$). For Br alone, there was no significant effect at any concentration. For PFAA alone and in combination with Br, there was significantly increased ROS production compared to DMSO control at $100\times$ and $500\times$ blood concentration (all $p < 2 \times 10^{-16}$ except PFAA + Br 100 x: $p < 0.001$). As may be seen from the plot, the estimates for luminescence in the PFAA + Cl mixture were larger than for each single mixture, however, we could not detect any interaction between the mixtures. Adding Br to the mixtures had little effect. Estimates for the PFAA + Cl mixture with or without Br added indicate that all combinations induced more luminescence than DMSO control both at $100\times$ and $500\times$ blood concentration (all $p < 2 \times 10^{-16}$).

3.1.2. Human lymphocytes

Also, in lymphocytes, the model indicated a clear positive

Table 2
Estimated model coefficients for the luminol mixed models.

Model coefficients/explanatory variables	Granulocytes				Lymphocytes				Monocytes			
	Coefficient[1]	95 % CI	p-value		Coefficient[1]	95 % CI	p-value		Coefficient[1]	95 % CI	p-value	
Intercept	226895.04100	[197479.32461, 260692.40277]	1.06×10^{-10}	***	1185.42350	[815.65735, 1722.81763]	4.15×10^{-8}	***	1454.00872	[1189.84835, 1776.81581]	2.58×10^{-9}	***
PFAA present	1.02365	[1.00938, 1.03813]	0.0964		1.01682	[0.95078, 1.08745]	0.8039		1.34986	[1.25963, 1.44655]	1.83×10^{-5}	***
Cl present	0.96537	[0.95191, 0.97902]	0.0124	*	1.03479	[0.96774, 1.10649]	0.6099		1.36971	[1.27671, 1.46949]	9.96×10^{-6}	***
Br present	0.96768	[0.95419, 0.98137]	0.0197	*	0.92936	[0.86896, 0.99395]	0.2760		1.28544	[1.19927, 1.37781]	3.33×10^{-4}	***
Mixture concentration	1.00010	[1.00005, 1.00014]	0.0279	*	1.00079	[1.00059, 1.00099]	8.44×10^{-5}	***	1.00094	[1.00073, 1.00116]	1.17×10^{-5}	***
Buffer control	1.02686	[1.00428, 1.04995]	0.2338		0.86316	[0.78513, 0.94894]	0.1210		1.20128	[1.08164, 1.33416]	0.081218	
Interaction PFAA/Cl	**1.00532**	**[0.99099, 1.01986]**	**0.7119**		**1.07317**	**[1.00158, 1.14987]**	**0.3068**		**0.78328**	**[0.72958, 0.84094]**	**6.45×10^{-4}**	***
Interaction PFAA/Br	**1.01178**	**[0.99736, 1.02641]**	**0.4150**		**1.17769**	**[1.09917, 1.26181]**	**0.0181**	*	**0.92783**	**[0.86425, 0.99609]**	**0.291969**	
Interaction Cl/Br	**1.03175**	**[1.01704, 1.04667]**	**0.0299**	*	**1.01140**	**[0.94400, 1.08361]**	**0.8695**		**0.80712**	**[0.75190, 0.86640]**	**0.002657**	**
Interaction PFAA/mixture conc.	1.00098	[1.00095, 1.00102]	$<2 \times 10^{-16}$	***	1.00163	[1.00147, 1.00179]	$<2 \times 10^{-16}$	***	1.00177	[1.00159, 1.00194]	$< 2.0 \times 10^{-16}$	***
Interaction Cl/mixture conc.	1.00066	[1.00062, 1.00069]	$<2 \times 10^{-16}$	***	1.00115	[1.00099, 1.00131]	3.00×10^{-12}	***	1.00164	[1.00147, 1.00181]	$< 2.0 \times 10^{-16}$	***
Interaction Br/mixture conc.	0.99996	[0.99992, 0.99999]	0.2446		0.99977	[0.99961, 0.99993]	0.1490		0.99955	[0.99938, 0.99972]	0.009168	**
AIC	−1164.4				569.4				329			
Number of observations	558				552				412			
Number of groups (persons)	6				8				6			

AIC = Akaike's information criterion, conc. = concentration, CI = confidence interval.
Note: Separate mixed linear regression models were derived for granulocytes, lymphocytes and monocytes. Coefficients for each explanatory variable with confidence intervals and *p*-value are shown. To derive the models, the outcome variable was log-transformed. To ease interpretation; the coefficients from the additive model on a logarithmic scale have been back-transformed to yield a multiplicative model. Coefficients higher than one indicate explanatory variables associated with an increase in luminescence; those below 1 indicate variables associated with a decrease in luminescence. *p*-values below 0.05 are construed as indicating a significant association between an explanatory variable and resulting luminescence. Terms shown in bold represent interactions between mixtures. Mixture concentration is a continuous variable; all other are dichotomous. To obtain an estimate from the multiplicative model, the coefficients of dichotomous variables or interaction terms containing such should be included only when dichotomous variables are true; i.e. when all mixtures relevant to a term are present. The first three coefficients may be construed as a shift of the intercept with the Y axis when each mixture is present, alone or in combinations. Original coefficients from the additive model on a log scale are provided in Supplementary Table S3, corresponding to β_0 through β_{11} given in Equation (1).
[1] Coefficient = exponentiated log value.

Table 3
Concentration-response coefficients with 95 % confidence interval.

Compound	Assay							
	Luminol						DCF	
	Granulocytes		Lymphocytes		Monocytes		Granulocytes	
	Estimate	CI	Estimate	CI	Estimate	CI	Estimate	CI
PFAA	1.083×10^{-3}	$[9.967 \times 10^{-4}, 1.168 \times 10^{-3}]$	2.422×10^{-3}	$[2.032 \times 10^{-3}, 2.812 \times 10^{-3}]$	2.707×10^{-3}	$[2.301 \times 10^{-3}, 3.114 \times 10^{-3}]$	5.520×10^{-5}	$[^-3.500 \times 10^{-5}, 1.450 \times 10^{-4}]$
Cl	7.570×10^{-4}	$[6.712 \times 10^{-4}, 8.429 \times 10^{-4}]$	1.945×10^{-3}	$[1.556 \times 10^{-3}, 2.335 \times 10^{-3}]$	2.580×10^{-3}	$[2.168 \times 10^{-3}, 2.993 \times 10^{-3}]$	5.75×10^{-5}	$[4.010 \times 10^{-5}, 7.480 \times 10^{-5}]$
Br	5.669×10^{-5}	$[-2.915 \times 10^{-5}, 1.425 \times 10^{-4}]$	0.560×10^{-3}	$[0.170 \times 10^{-3}, 0.950 \times 10^{-3}]$	4.915×10^{-4}	$[8.438 \times 10^{-5}, 8.985 \times 10^{-4}]$	-1.03×10^{-4}	$[-1.650 \times 10^{-4}, -4.040 \times 10^{-5}]$

Estimate: Increase/decrease in log luminescence/fluorescence per increase in unit concentration, CI = 95 % confidence interval.
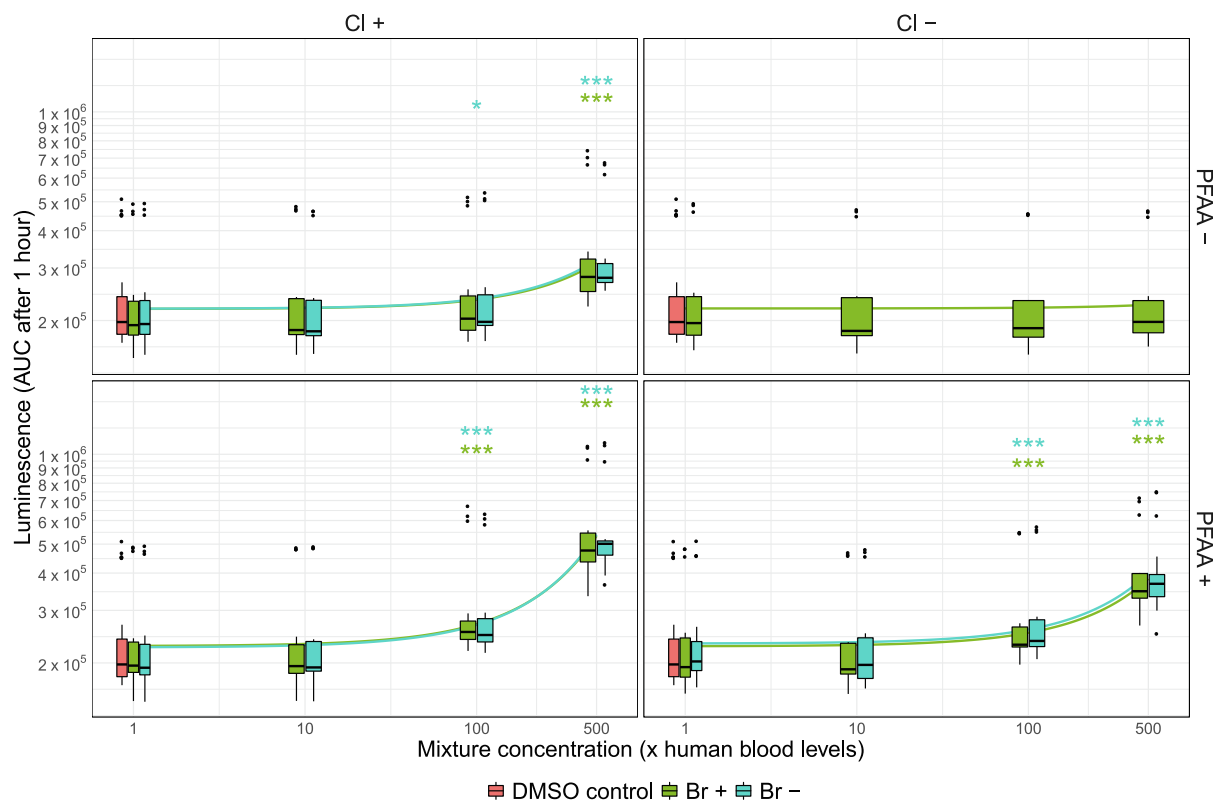

Fig. 1. Absolute luminescence values as a measure of ROS production in isolated human neutrophils measured by the luminol assay. Values were calculated as area under the curve (AUC) after 1 h exposure to 1, 10, 100 and 500× the concentration in human blood of the PFAA, Br, Cl, PFAA + Cl, PFAA + Br and Br + Cl sub-mixtures, as well as the total (PFAA + Br + Cl) mixture, n = cells from 6 different persons. Concentration-response curves were obtained using a linear mixed model. Box plots represent the spread of the raw data at tested concentrations. Each panel shows a combination of sub-mixtures with (green) and without (light blue) Br. The presence or absence of PFAA or Cl is indicated with + or −. Each box-plot spans from the first to the third quartile, the solid line on the box represents the median. Upper whiskers show the third quartile plus 1.5× the interquartile range (IQR), lower whiskers the first quartile minus 1.5× IQR. Points outside the whiskers indicate outliers beyond the whisker range. Significant differences between predicted mean values at tested concentrations of the mixtures and DMSO control are indicated with *, and *** for p < 0.05 and p < 0.001, respectively. PFAA = perfluorinated compounds, Br = brominated compounds, Cl = chlorinated compounds. Values are plotted on a logarithmic scale. (For interpretation of the references to colour in this figure legend, the reader is referred to the web version of this article.)

concentration–response relationship for the PFAA ($p < 0.001$) and Cl ($p < 0.001$) mixtures, and a slightly positive relationship for Br ($p < 0.005$) (Table 3). There was interaction between the PFAA and the Br mixtures ($p < 0.05$), indicating a synergistic effect in the mixtures containing both (PFAA + Br/total mixture). For model coefficients, see Table 2. Fig. 2 shows the estimated concentration–response curves for each combination of mixtures, as well as results from post-hoc hypothesis tests comparing each mixture combination with DMSO control. The Cl mixture induced significantly more luminescence at 100× ($p < 0.01$) and 500× ($p < 2 \times 10^{-16}$) human blood levels, whereas the combined Br + Cl mixture had significant impact only at 500× human blood levels (p

$< 2 \times 10^{-16}$). For the Br mixture alone, there was no significant effect at any concentration. For the PFAA mixture alone, there was a difference from DMSO control at 100× ($p < 0.001$) and 500× ($p < 2 \times 10^{-16}$) human blood levels, whereas for PFAA + Br the difference was again only significant at the highest concentration ($p < 2 \times 10^{-16}$). As may be observed from the plot, the estimates for luminescence at the two highest concentrations for the PFAA + Cl mixture were larger than for each single mixture. However, no interaction could be detected between the mixtures ($p = 0.31$). Adding Br to the mixtures at these concentrations had little effect, and the estimates for the PFAA + Cl mixture with or without Br indicated that all combinations induced more
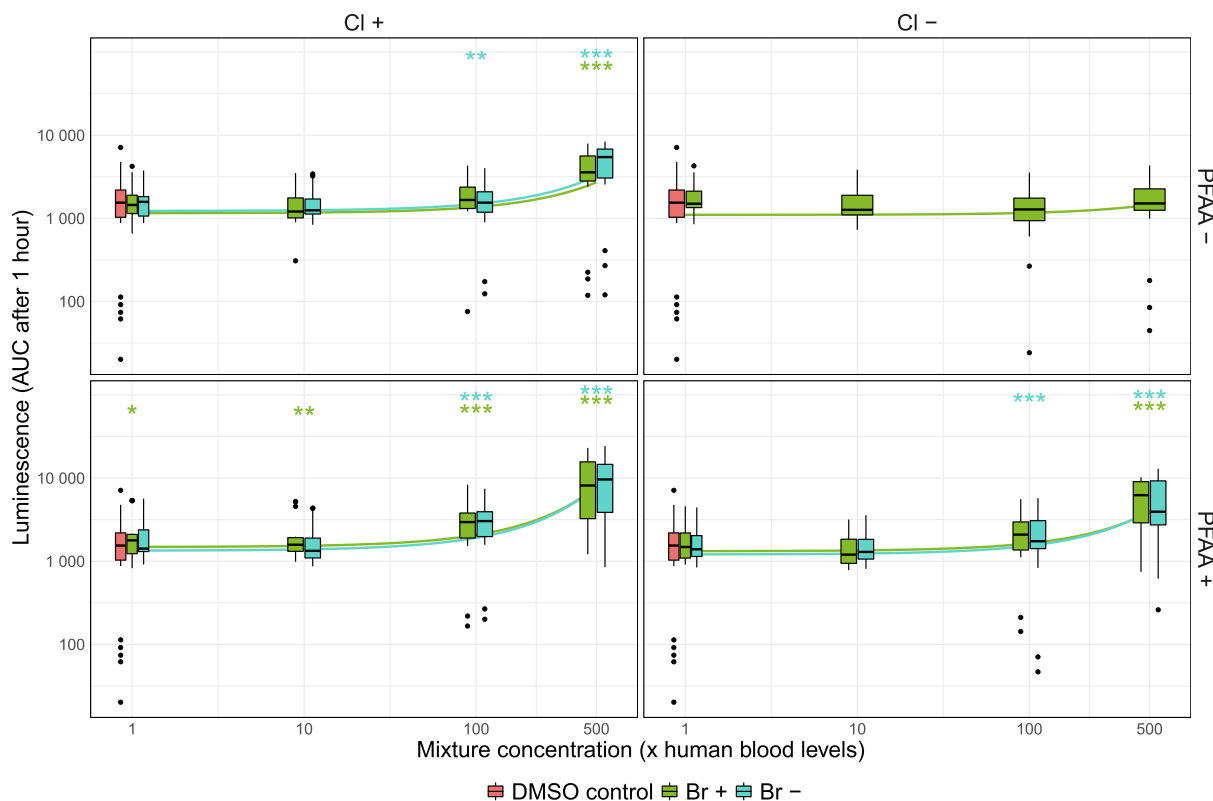
Fig. 2. Absolute luminescence values as a measure of ROS production in isolated human lymphocytes measured by the luminol assay. Values were calculated as area under the curve (AUC) after 1 h exposure to 1, 10, 100 and 500× the concentration in human blood of the PFAA, Br, Cl, PFAA + Cl, PFAA + Br and Br + Cl sub-mixtures, as well as the total (PFAA + Br + Cl) mixture, n = cells from 8 different persons. Concentration-response curves were obtained using a linear mixed model. Box plots represent the spread of the raw data at the tested concentrations. Each panel shows a combination of sub-mixtures with (green) and without (light blue) Br. The presence or absence of PFAA or Cl is indicated with + or −. Each box-plot spans from the first to the third quartile, the solid line on the box represents the median. Upper whiskers show the third quartile plus 1.5× the interquartile range (IQR), lower whiskers the first quartile minus 1.5× IQR. Points outside the whiskers indicate outliers beyond the whisker range. Significant differences between predicted mean values at tested concentrations of the mixtures and DMSO control are indicated with *, ** and *** for p < 0.05, p < 0.01 and p < 0.001, respectively. PFAA = perfluorinated compounds, Br = brominated compounds, Cl = chlorinated compounds. Values are plotted on a logarithmic scale. (For interpretation of the references to colour in this figure legend, the reader is referred to the web version of this article.)

luminescence than the DMSO control at 100× and 500× human blood levels (all $p < 2 \times 10^{-16}$). At the lower concentrations, 10× and 1× human blood levels, only the total mixture (PFAA + Cl combined with Br) induced significantly more luminescence than DMSO ($p < 0.05$ and $p < 0.01$), whereas no difference could be detected here for the PFAA + Cl mixture.

3.1.3. Human monocytes

For the monocytes, as for the other cell types, there was a clear significant positive concentration–response in luminescence for both PFAA and Cl mixtures ($p < 0.001$ for both), whereas clearly less pronounced for the Br mixture ($p < 0.05$) (Table 3). There was a significant negative interaction between the PFAA and Cl mixture ($p < 0.001$) and between the Br and Cl mixture ($p < 0.01$), indicating antagonism in mixtures containing these combinations of compounds (PFAA + Cl, Br + Cl and total mixture). Model coefficients are shown in Table 2. All 7 mixture combinations significantly increased luminescence compared to DMSO control even at concentrations corresponding to human blood levels. Fig. 3 shows concentration–response curves for the various mixtures, as well as *p*-values for difference from DMSO control at each tested concentration.

3.2. Mixture-induced ROS production assessed with the DCF assay.

Also, in the DCF assay, there was a positive concentration–response relationship in fluorescence in neutrophils for the Cl ($p < 0.001$) and

PFAA mixtures, although not reaching significance for PFAA ($p = 0.33$). For the Br mixture, the concentration–response correlation was negative ($p < 0.001$) (Table 3). There was positive interaction between PFAA and Cl ($p < 6 \times 10^{-15}$) and between PFAA and Br ($p < 0.01$). This indicates that fluorescence was higher for the mixtures containing both groups (PFAA + Cl, PFAA + Br and total mixture) than the sum of predicted effects of each mixture alone. Model coefficients are in Table 4.

Comparing fluorescence values for different mixtures with DMSO control, no significant effects were detected for the Cl mixture alone or in combination with Br. The Br mixture on its own, however, induced significantly less fluorescence than DMSO control at 100× ($p < 0.01$) and 1000× ($p < 3 \times 10^{-7}$) human blood levels. The PFAA mixture alone had no significant impact, whereas the combined PFAA + Br mixture induced significantly more fluorescence at 1000× human blood levels ($p < 8 \times 10^{-5}$). The combined PFAA + Cl mixture induced an increase at 1000× human blood levels ($p < 2 \times 10^{-16}$). Using the total PFAA + Cl + Br mixture, fluorescence was significantly higher than DMSO control at 100× ($p < 0.05$) and 1000× ($p < 2 \times 10^{-16}$) human blood levels.

3.3. Mechanistic studies of mixture-induced ROS production in human neutrophils

3.3.1. Effects of β-adrenergic receptor antagonists on mixture-induced and basal ROS

Co-incubation of human neutrophils with the total (PFAA + Br + Cl) mixture and various antagonist of the β2AR resulted in significant
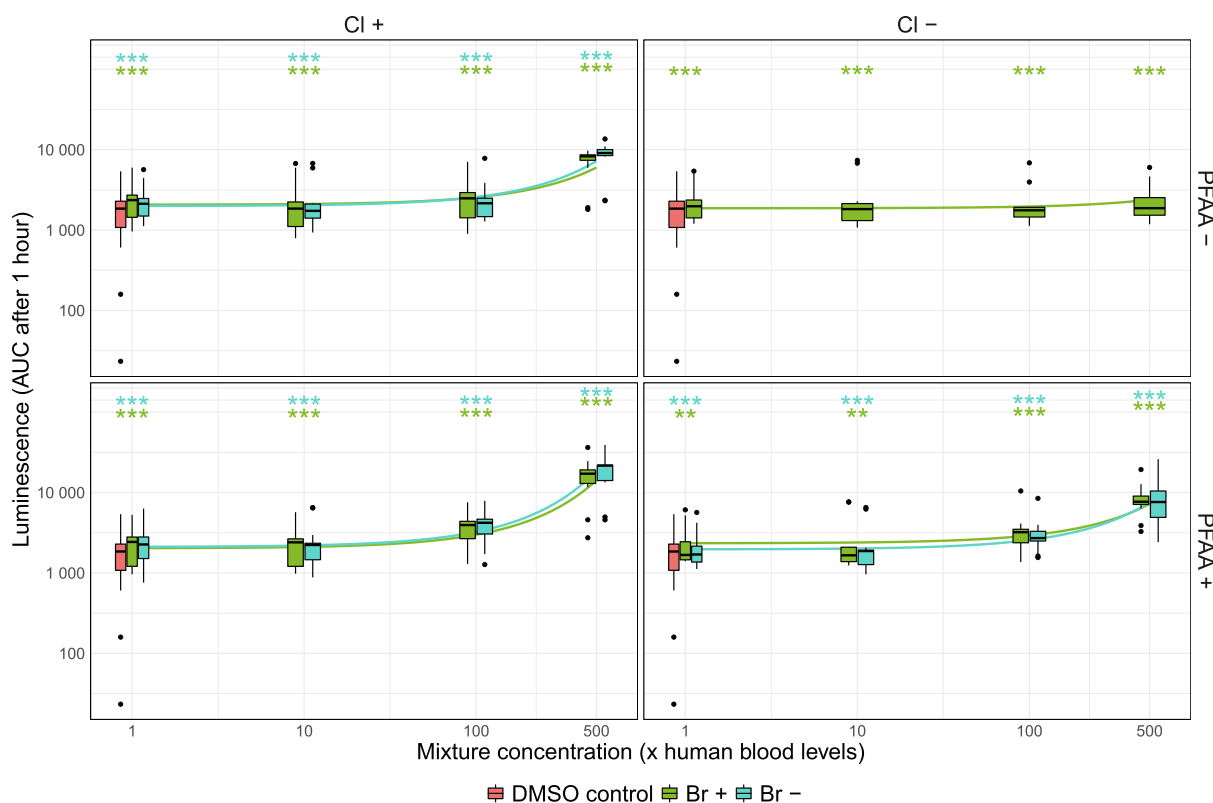
Fig. 3. Absolute luminescence values as a measure of ROS production in isolated human monocytes measured by the luminol assay. Values were calculated as area under the curve (AUC) after 1 h exposure to 1, 10, 100 and 500× the concentration in human blood of the PFAA, Br, Cl, PFAA + Cl, PFAA + Br and Br + Cl sub-mixtures, as well as the total (PFAA + Br + Cl) mixture, n = cells from 6 different persons. Concentration-response curves were obtained using a linear mixed model. Box plots represent the spread of the raw data at the tested concentrations. Each panel shows a combination of sub-mixtures with (green) and without (light blue) Br. The presence or absence of PFAA or Cl is indicated with + or −. Each box-plot spans from the first to the third quartile, the solid line on the box represents the median. Upper whiskers show the third quartile plus 1.5× the interquartile range (IQR), lower whiskers the first quartile minus 1.5× IQR. Points outside the whiskers indicate outliers beyond the whisker range. Significant differences between predicted mean values at tested concentrations of the mixtures and DMSO control are indicated with *, ** and *** for $p < 0.05$, $p < 0.01$ and $p < 0.001$, respectively. PFAA = perfluorinated compounds, Br = brominated compounds, Cl = chlorinated compounds. Values are plotted on a logarithmic scale. (For interpretation of the references to colour in this figure legend, the reader is referred to the web version of this article.)

reductions in cumulative luminescence as a measure of ROS production, as compared to treatment with the mixture alone (Fig. 5). More specifically, ICI reduced ROS production with 27 ± 5, 64 ± 8, and 98 ± 6 % at concentrations of 10, 50 and 100 μM ($p < 0.001$ for all), propranolol reduced ROS production with 14 ± 7 and 17 ± 6 % at 1 and 10 μM ($p < 0.01$, and $p < 0.001$, respectively) and carvedilol reduced ROS with 52 ± 5 % at 10 μM ($p < 0.001$). No effect was seen for 1 μM carvedilol. Furthermore, 10 and 50 μM ICI reduced ROS production with 31 ± 16 and 58 ± 21 % for the Cl-mixture ($p < 0.01$, and $p < 0.001$, respectively) and 20 ± 9 and 56 ± 11 % for the PFAA + Cl mixture ($p < 0.001$ for both). 50 μM ICI reduced PFAA-induced ROS production with 51 ± 12 % ($p < 0.001$), whereas 10 μM ICI had no significant effect. Finally, 10 μM carvedilol significantly reduced the Cl-, PFAA- and PFAA + Cl-induced ROS production with 48 ± 16, 34 ± 11 and 42 ± 9 %, respectively ($p < 0.001$ for all). Some of the antagonists also affected basal ROS production in DMSO treated cells. For ICI, ROS production was reduced with 46 ± 18 and 40 ± 22 % for 10 and 50 μM ($p < 0.001$ for the former and $p < 0.01$ for the latter), whereas 100 μM ICI caused almost complete obliteration of ROS production ($p < 0.001$). 10 μM carvedilol and propranolol significantly reduced basal ROS production with 74 ± 17 and 29 ± 18 %, respectively ($p < 0.001$ for the former, and $p < 0.05$ for the latter). No significant effect was seen for 1 μM of the same two antagonists. As may be seen from Fig. 5, although some reductions in basal ROS production could be observed in DMSO treated cells with a few of the antagonists, the reductions in absolute luminescence values for the total mixture treated cells largely exceeded the reductions in the DMSO

controls. This was also the case for the PFAA + Cl mixture, whereas for the Cl mixture the absolute reductions induced by 10 μM carvedilol and 10 μM ICI were at a similar level or were slightly exceeded by the reductions in basal ROS production in the DMSO treated cells (100 714 vs 105 107 for the first, and 64 882 vs 66 071 for the latter). For the PFAA mixture the decrease after co-treatment with 10 μM carvedilol was somewhat exceeded by the reduction in basal luminescence (91 524 vs 105 107).

3.3.2. Effects of β-adrenergic receptor agonists on total mixture-induced and basal ROS

Interestingly, treatment of cells with increasing concentrations of the two β-adrenergic receptor agonists isoproterenol and salmeterol also significantly reduced total mixture-induced ROS production. 0.5, 1 and 10 μM isoproterenol reduced ROS with 28 ± 8, 28 ± 7 and 48 ± 7 % ($p < 0.001$ for all), whereas 0.1, 1 and 10 μM salmeterol caused reduction in ROS of 21 ± 8, 23 ± 7 and 51 ± 7 % ($p < 0.001$ for all). The two agonists did not significantly affect basal ROS production in DMSO-treated controls.

3.3.3. Effects of NADPH-oxidase inhibition and intracellular calcium chelation on ROS production

Treatment of cells with 5 μM of the intracellular calcium-chelator BAPTA-AM caused significant reductions in ROS after co-treatment with all the four tested mixtures, with decreases of 34 ± 16, 24 ± 11, 30 ± 9 and 44 ± 4 % for the Cl, PFAA, PFAA + Cl and total mixtures,

Table 4
Estimated model coefficients for the DCF generalised estimating equation.

Model coefficients/explanatory variables	Neutrophils			
	Coefficient[1]	95 % CI	*p*-value	
Intercept	22295098878.51950	[21556696523.20277, 23058794443.19930]	$<2 \times 10^{-16}$	***
PFAA present	0.98155	[0.94729, 1.01705]	0.05087	
Cl present	0.97313	[0.93917, 1.00833]	0.09590	
Br present	0.97897	[0.94480, 1.01438]	0.03911	*
Mixture concentration	0.99988	[0.99983, 0.99993]	3.18×10^{-5}	***
Buffer control	1.07057	[1.01466, 1.12957]	0.12648	
Interaction PFAA/Cl	**1.06594**	**[1.03057, 1.10252]**	**6.22×10^{-15}**	***
Interaction PFAA/Br	**1.01849**	**[0.98469, 1.05344]**	**0.00548**	**
Interaction Cl/Br	**1.02076**	**[0.98689, 1.05579]**	**0.09332**	
Interaction PFAA/mixture conc.	1.00017	[1.00013, 1.00021]	$<2 \times 10^{-16}$	***
Interaction Cl/mixture conc.	1.00017	[1.00014, 1.00021]	6.30×10^{-12}	***
Interaction Br/mixture conc.	1.00001	[0.99998, 1.00005]	0.10136	
Number of observations	359			
Number of groups (persons)	4			

Note: Coefficients for each explanatory variable with confidence intervals and *p*-value are shown. To derive the model, the outcome variable was log-transformed. To ease interpretation; the coefficients from the additive model on a logarithmic scale have been back-transformed to yield a multiplicative model. Coefficients higher than one indicate explanatory variables associated with an increase in fluorescence; those below 1 indicate variables associated with a decrease in fluorescence. *p*-values below 0.05 are construed as indicating a significant association between an explanatory variable and resulting fluorescence. Terms shown in bold represent interactions between mixtures. Mixture concentration is a continuous variable; all other are dichotomous. To obtain an estimate from the multiplicative model, the coefficients of dichotomous variables or interaction terms containing such should be included only when dichotomous variables are true; i.e. when all mixtures relevant to a term are present. The first three coefficients may be construed as a shift of the intercept with the Y axis when each mixture is present, alone or in combinations. Original coefficients from the additive model on a log scale are provided in Supplementary Table S4.

CI = confidence interval.

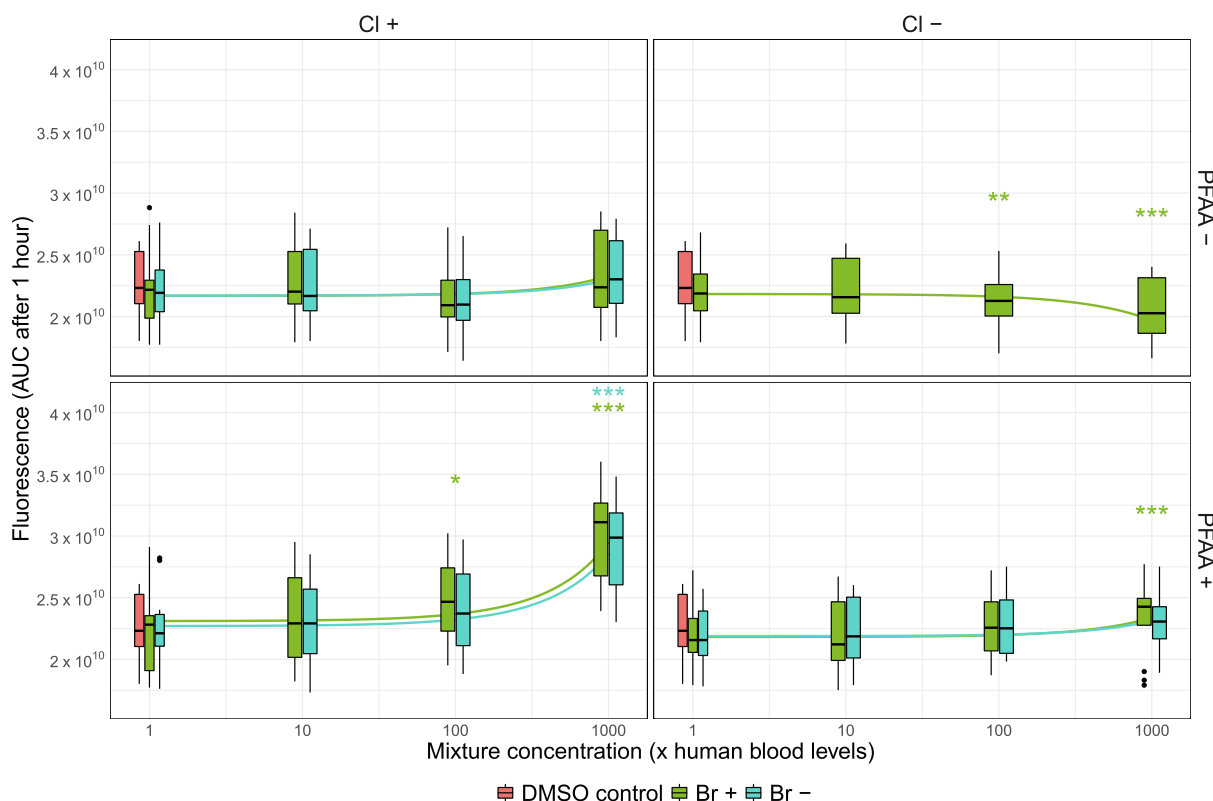[1] Coefficient = exponentiated log value.

Fig. 4. Absolute fluorescence values as a measure of ROS production in isolated human neutrophils measured by the DCF assay. Values were calculated as area under the curve (AUC) after 1 h exposure to 1, 10, 100 and 1000× the concentration in human blood of the PFAA, Br, Cl, PFAA + Cl, PFAA + Br and Br + Cl sub-mixtures, as well as the total (PFAA + Br + Cl) mixture, n = cells from 4 different persons. Concentration-response curves were obtained using a generalised estimating equation. Box plots represent the spread of the raw data at the tested concentrations. Each panel shows a combination of sub-mixtures with (green) and without (light blue) Br. The presence or absence of PFAA or Cl is indicated with + or −. Each box-plot spans from the first to the third quartile, the solid line on the box represents the median. Upper whiskers show the third quartile plus 1.5× the interquartile range (IQR), lower whiskers the first quartile minus 1.5× IQR. Points outside the whiskers indicate outliers beyond the whisker range. Significant differences between predicted mean values at tested concentrations of the mixtures and DMSO control are indicated with *, ** and *** for p < 0.05, p < 0.01 and p < 0.001, respectively. PFAA = perfluorinated compounds, Br = brominated compounds, Cl = chlorinated compounds. (For interpretation of the references to colour in this figure legend, the reader is referred to the web version of this article.)

respectively ($p < 0.01$ for the first and $p < 0.001$ for the three last). 1 μM BAPTA-AM had no effect on total mixture-induced ROS production. 0.1 μM of the NADPH-oxidase inhibitor DPI significantly reduced mixture-induced ROS production after treatment with all the four mixtures. The reductions were 26 ± 16, 49 ± 11, 53 ± 9 and 65 ± 5 % for the Cl, PFAA, PFAA + Cl and total mixtures, respectively ($p < 0.05$ for the first and $p < 0.001$ for the three last). Furthermore, 1 μM DPI caused almost complete obliteration of ROS production in total mixture treated cells ($p < 0.001$). Both BAPTA-AM and DPI also significantly affected ROS production in DMSO-treated controls with reductions of, 51 ± 17, 71 ± 17 and 51 ± 18 % for 1 and 5 μM BAPTA-AM and 0.1 DPI, respectively ($p < 0.001$ for all). 1 μM DPI caused almost complete obliteration of ROS production ($p < 0.001$). As mentioned above for the β2AR antagonist, the reductions in absolute luminescence values after treatment with DPI and BAPTA-AM for most mixtures exceeded the reductions in the luminescence values observed for the DMSO controls. The few exceptions were 5 μM BAPTA-AM in conjunction with the Cl and PFAA mixtures and 0.1 μM DPI together with the Cl mixture, where the reductions in the DMSO control slightly exceeded those seen for these modulator-mixture combinations, with decreases of 70 692 and 63 934 vs. 100 802 in the control for the two first, and 54 627 vs. 72 333 for the latter (Fig. 5).

3.3.4. Effects on the aryl hydrocarbon receptor (AhR)

No significant effects on total mixture-induced ROS production could be observed after co-treatment of cells with the mixture and the AhR antagonist CH-223191 or the agonist betanaphthoflavone. Similarly, these chemicals did not affect basal ROS production in DMSO-treated cells (Fig. 5).

3.4. Total mixture-induced effects on cAMP levels

β2ARs signal partly via cAMP. Thus, to further assess the potential activation of βARs, we explored effects on cAMP levels (n = cells from 7 different persons). Isolated human neutrophils were exposed to the total mixture for 15 and 30 min. The non-selective βAR agonist isoproterenol was used as positive control. Both the total mixture and isoproterenol induced statistically significant and comparably large increases in cAMP at both the examined time points (Fig. 6). On average, the mixture-exposure induced a 19 % increase in cAMP after 15 min (non-significant) and a 24 % increase after 30 min, while isoproterenol-exposure induced a 23 % increase after 15 min and a 20 % increase after 30 min. Furthermore, an increase in cAMP levels after exposure to the total mixture was observed at both time points in cells from all donors, except one. Importantly, in cells from this non-responding donor the positive control, isoproterenol, failed to increase cAMP levels, but rather reduced levels compared to the control after both 15- and 30-min exposure (not shown). Preliminary studies showed that the β2AR antagonist ICI-118551 (100 μM), caused approximately 40 % reduction in cAMP levels induced after 30 min exposure to the total mixture, while the β2AR antagonist caused a corresponding increase in cAMP at the earlier time point (Supplementary Fig. S5).

3.5. LDH assay

No significant damage to the granulocyte cell membrane could be detected using the LDH assay after 2 h exposure to 100 and 500× of the PFAA, Cl, PFAA + Cl or total mixture (data not shown).

4. Discussion

In the present study we show that mixtures of halogenated POPs relevant to human environmental exposure induce ROS production *in vitro* in the three forms of human leucocytes most prevalent in peripheral blood, pertaining both to myeloid and lymphoid lines. Results from experiments with pharmacological modulators suggest involvement of the β2AR, cAMP, as well as Ca^{2+} and NADPH-oxidase in mixture-induced ROS production in neutrophils. LDH assay in neutrophils further indicated that the mixture-induced ROS production was a result of activation and production of ROS in viable cells.

4.1. POP-induced ROS production in neutrophils: Potential mechanisms of action

Mechanistic studies in neutrophils, applying pharmacological modulators, indicated that similar mechanisms for ROS production may be present after exposure to the single Cl and PFAA-, the combined PFAA + Cl, and the total mixtures (Fig. 5). In all cases, the β2AR, intracellular Ca^{2+}, and NADPH oxidase seemed to be involved. Some of the modulators also affected basal ROS production. As previously discussed in Berntsen et al. (2016) and Berntsen et al. (2017), one cannot rule out that some activation of neutrophils may occur during the isolation process, resulting in ROS production through similar mechanisms as after mixture exposure. However, the decreases in ROS production after modulator treatment in unstimulated cells were considerably smaller than the decreases in total mixture-treated and mostly also in sub-mixture-treated cells (Fig. 5). This indicates that modulator effects would not be due to action on basal ROS only, but also on mixture-induced ROS production.

There exists extensive evidence of a crucial role for adrenergic mechanisms in the regulation of innate immunity. In human neutrophils, adrenaline and noradrenaline inhibit migration, CD11b/CD18 expression, and oxidative metabolism, possibly through βAR signalling (Scanzano and Cosentino, 2015). Exposure to the POP mixture induced NADPH oxidase-dependent ROS formation, which appeared to be dependent of the β2AR, as three different antagonists inhibited this response (Fig. 5). The POP mixture also increased cAMP formation in neutrophils to a level comparable with the non-selective βAR-agonist isoproterenol, further indicating that POP-exposure may actually activate βARs (see Fig. 7). In addition, preliminary studies showed that the β2AR antagonist ICI-118551, reduced cAMP levels after 30 min exposure to the total mixture, while it caused a corresponding increase in cAMP after 15 min (Supplementary Fig. S5). The reason for this biphasic effect of ICI-118551 remains unclear. The role of toll-like receptors (TLR), especially TLR4, in radical cycling induced by environmental pollutants is well established (Lucas and Maes, 2013). Conceivably, the observed involvement of β2AR in POP-induced ROS, could also involve crosstalk with TLR-signalling as has been reported for TLR4 (Kizaki et al., 2008). To our knowledge, this is the first study indicating that also POPs may interfere with adrenergic pathways and extends previous reports of interactions between PAHs and β2AR (Bernstein et al., 2011; Cazzola et al., 2011; Mayati et al., 2012; Mayati et al., 2014; Scanzano and Cosentino, 2015; Mayati et al., 2017). Moreover, the involvement of the β2AR in pollutant-induced respiratory burst in human neutrophils also represents a novel finding. Although the mechanisms of these responses remain to be clarified, studies in other tissues support our findings by showing that mice with transgenic β2AR overexpression provoked NADPH oxidase-derived ROS production in the heart (Xu et al., 2011). This was mainly caused by up-regulation of reduced NADPH oxidase (Nox) 2 and 4 and accompanied by p38 mitogen-activated protein kinase activation, fibrosis, apoptosis and cardiac dysfunction (Di Lisa et al., 2011).

In our study, in contrast to the POP mixtures, exposure to the selective β2AR agonist salmeterol and the non-selective βAR-agonist isoproterenol did not lead to ROS formation, but rather inhibited ROS production. This resembles previous studies reporting that β2AR agonists suppress ROS-generation in neutrophils (Opdahl et al., 1993; Barnett et al., 1997). Thus, the observed β2AR-dependency of the POP-mixture induced ROS-response may appear somewhat contradictory. However, it should be emphasised that G protein-coupled receptor (GPCR)-signalling is highly complex and does not operate in a simple two-state (on/off) mode. Activation/inactivation involves both
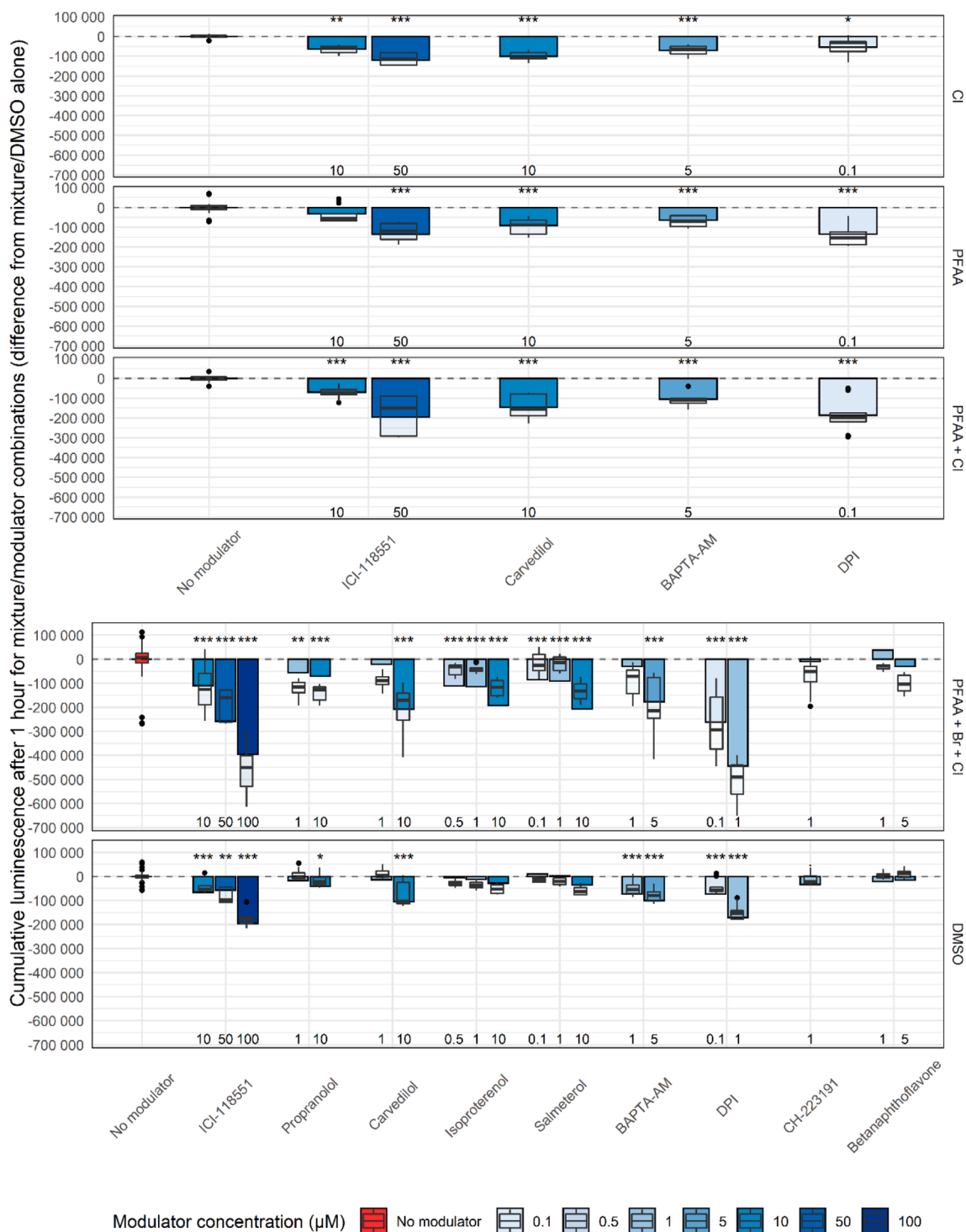
Fig. 5. Estimated mean reduction in cumulative luminescence after one h in different POP mixture/pharmacological modulator combinations and DMSO control/modulator combinations. Each panel shows data for DMSO control (second panel from top, right side) or one mixture (remaining panels) with and without modulators (n = cells from 3 to 11 persons for the total mixture and DMSO control, and 3–6 for the Cl, PFAA and PFAA + Cl mixtures). Coloured bars show estimate for mean reduction from luminescence levels in DMSO or POP mixture alone, modelled using a linear mixed model. Deeper blue shades indicate increasing concentration. Horizontal dashed lines show mean cumulative luminescence levels in mixtures without modulators/DMSO control. Values for modulators tested with each POP mixture and DMSO control are shown along the X axis of each panels. Boxplot overlays show quantiles of raw data distribution in each group, leftmost boxplots in each panel show raw data quantiles for each mixture/DMSO without modulators (in red). Each box-plot spans from the first to the third quartile, the solid line on the box represents the median. Upper whiskers show the third quartile plus 1.5× the interquartile range (IQR), lower whiskers the first quartile minus 1.5× IQR. Points outside the whiskers indicate outliers beyond the whisker range. Significant reduction in cumulative luminescence in mixture/modulator and DMSO/modulator combinations compared with mixture/DMSO alone are indicated with *, ** and *** for p < 0.05, p < 0.01 and p < 0.001, respectively. All data in original luminescence units. (For interpretation of the references to colour in this figure legend, the reader is referred to the web version of this article.)
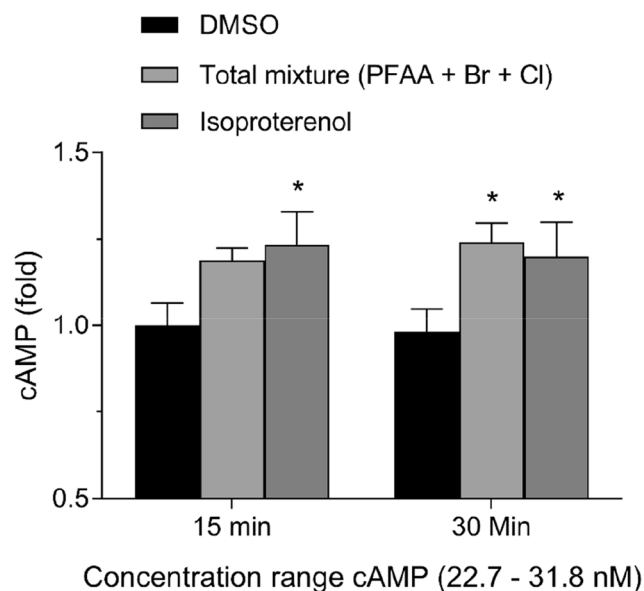
Fig. 6. Alteration in intracellular cAMP levels in isolated human neutrophils. Cells from individual donors were exposed to the total mixture (PFAA + Br + Cl) at 500× human blood levels or isoproterenol (1 μM) as positive control. cAMP concentrations were measured in cell lysates as described under Materials and methods. *Significantly different from vehicle (DMSO) controls (p < 0.05), n = cells from 6 to 7 different persons.

traditional (orthosteric) interactions at the ligand binding pocket as well as allosteric activation/modulation through interactions with other parts of the receptor structure, and multiple receptor configurations

allows a continuum of different signalling outcomes from GPCR ligation (Salon et al., 2011). It remains to clarify the precise role of β2AR in POP-induced ROS-formation, but an intriguing possibility is that persistent β2AR-activation may be required to induce oxidative stress, as pointed out by others (Rambacher and Moniri, 2020). It is also suggested that there might be a reciprocal interplay between the β2AR and ROS, with self-regulation of signalling efficacy and ligand binding, that may be unfavourably altered in pathological states (Rambacher and Moniri, 2020).

It is well known that β2AR stimulation by agonists commonly leads to activation of AC via Gs proteins and subsequently increases the production of cAMP (Deupi and Kobilka, 2010), known to directly activate protein kinase A (PKA) and phosphodiesterases. Phosphodiesterases catalyse the hydrolysis of the 3′ cyclic phosphate bond of cyclic nucleotides like cAMP (Gimenez et al., 2015) (see Fig. 7). Although the mechanisms behind a possible desensitisation of β2ARs after exposure to the two agonists salmeterol and isoproterenol in our study are unknown, we speculate that this may depend on either retrograde phosphorylation and inhibition of the β2AR (Gimenez et al., 2015), or by a Ca^{2+}-dependent mechanism as suggested for PAHs (Mayati et al., 2012). In a previous study, BaP was found to bind to β2ARs *in vitro* and to consequently activate a G protein/adenylyl cyclase/cAMP/Epac-1/IP3 pathway, which in turn resulted in increased intracellular Ca^{2+} from endoplasmic reticulum (ER) (Mayati et al., 2012). Also, a mixture of brominated flame retardants induced respiratory burst in human neutrophils *in vitro* via PI3kinase and intracellular Ca^{2+} release (Reistad and Mariussen, 2005). One potential hypothesis may thus be that the inhibition of POP-induced ROS formation by BAPTA-AM in our study may be due to chelation of Ca^{2+} release from ER, and subsequently decreased activation of MAP kinases like p38 (Di Lisa et al., 2011; Futosi et al., 2013) and ERK upstream of the NADPH oxidase. This is in line with
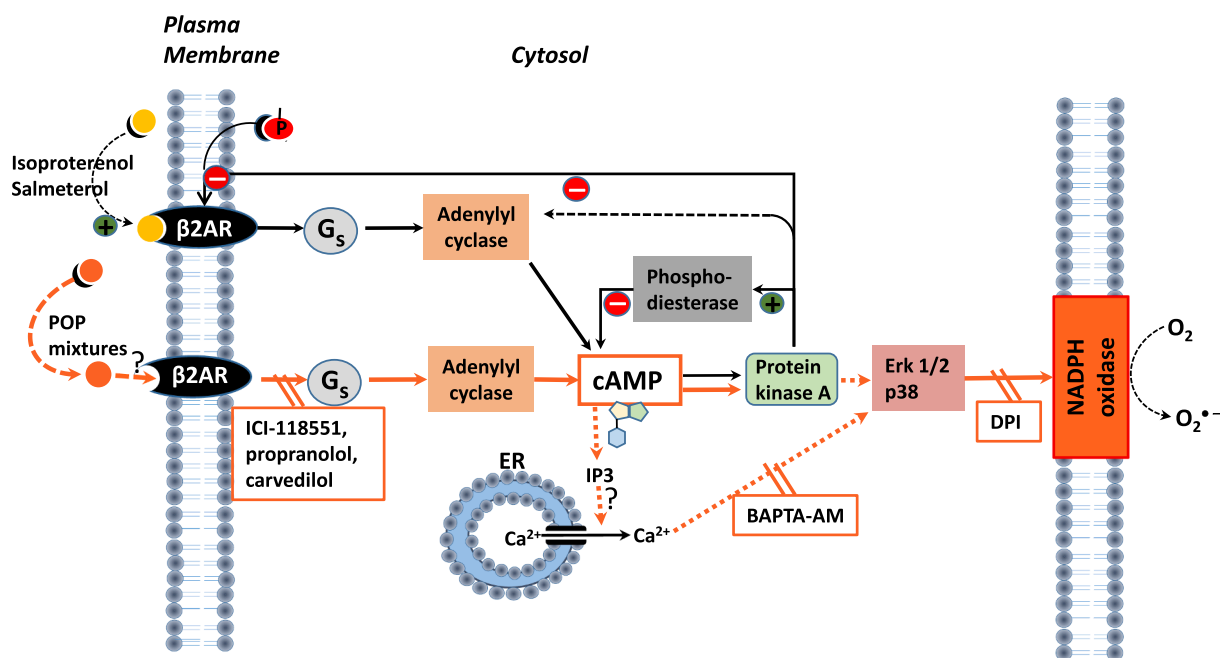

Fig. 7. Putative mechanisms for possible involvement of β2AR signalling pathways in ROS formation from the NADPH oxidase complex in human neutrophils after exposure to the POP mixtures (orange arrows and boxes illustrate endpoints measured or pharmacological modulators used, question marks or stippled lines indicate speculative mechanisms). A potent NADPH oxidase dependent ROS formation was inhibited by the β2AR antagonists ICI-118551, propranolol, and carvedilol. DPI inhibited ROS formation, showing that the NADPH oxidase was the primary source of ROS. The POP mixture and the β2AR agonist isoproterenol increased formation of intracellular cAMP, known to activate protein kinase A. The Gs (stimulatory G protein)-adenylyl cyclase-protein kinase A pathway may on one hand lead to phosphorylation of the β2AR and partial uncoupling (and inhibition), and phosphodiesterase activation. Phosphodiesterases catalyse the hydrolysis of the 3′ cyclic phosphate bond of cyclic nucleotides like cAMP. Activation of β2AR-cAMP-protein kinase A pathway may alternatively lead to release of Ca^{2+} from endoplasmic reticulum (ER) and further activation of p38 and Erk1/2 MAPK, resulting in assembly of the NADPH oxidase complex and ROS formation. In contrast to the POP mixtures, salmeterol and isoproterenol did not induce ROS formation in the neutrophils, possibly due to retrograde phosphorylation and inhibition of the β2AR (Gimenez et al., 2015). (For interpretation of the references to colour in this figure legend, the reader is referred to the web version of this article.)

previous studies where ERK1/2 kinases and p38MAPK were involved in ROS formation in neutrophils exposed *in vitro* to a mixture or single congeners of PCBs (Myhre et al., 2009; Berntsen et al., 2016). Co-exposure of cells to the POP mixture with the NADPH oxidase inhibitor DPI (Buck et al., 2019) diminished most of the ROS formation, showing that activation of the NADPH oxidase was the major source of the ROS formation in neutrophils after exposure to the total mixture (Figs. 5 and 7).

4.2. Mixture-induced ROS production in leucocytes:

We have previously shown that ROS production was induced in human neutrophils after exposure to the single PCB congeners 52, 153 and 180 from 2.5 μM and above (Berntsen et al., 2016) and that the PCB mixture Arochlor 1242 induced ROS production from 6 μM and above (Myhre et al., 2009). Further, DCF-detected NADPH oxidase-dependent ROS production has been reported in the human monocytic cell line THP-1 after treatment with 10 μM *trans*-nonachlor and dieldrin (Mangum et al., 2015). For *trans*-nonachlor no response was observed at a concentrations below 2.5 μM. p,p'-DDE had no effect on ROS production even at a concentration of 10 μM (Mangum et al., 2015). In Reistad and Mariussen (2005) the BDE mixture DE-71 induced significant ROS production assessed by lucigenin-amplified chemiluminescence from 4 μM and above; whereas no effects were detected using the luminol or DCF assays, indicating that ROS production was primarily extracellular (Reistad and Mariussen, 2005). Also, the single congener BDE-47 induced ROS production from 6 μM and above, whereas commercial mixtures of octaBDE and decaBDE, as well as HBCD had no effects (Reistad and Mariussen, 2005). For the perfluorinated compounds, Zarei et al. (2018) found PFOS-induced DCF-detected ROS production in isolated human lymphocytes at concentrations from 150 μM and 75 μM and above after 2 and 4 h exposure; respectively, but not at lower concentrations.

We have previously reported that luminol in neutrophils is made chemiluminescent by HOCl, but not by nitric oxide (NO•) or •OH. DCFH, on the other hand, was sensitive towards oxidation by $ONOO^-$, H_2O_2 (in combination with cellular peroxidases) and •OH, whilst not suitable for measurement of NO•, HOCl, or $O_2^{\bullet-}$ in biological systems (Myhre et al., 2003). In neutrophils and monocytes, the myeloperoxidase (MPO) system efficiently uses H_2O_2, generated from the NADPH oxidase system, and chloride to generate the potent oxidant HOCl with a strong bactericidal action *in vitro* (Harrison and Schultz, 1976). When monocytes are released into the circulation, they turn off MPO synthesis, which is further downregulated during their differentiation into macrophages (Tobler et al., 1988; Gullberg et al., 1999; Okada et al., 2016). However, although neutrophils and macrophages, the terminal forms of myeloid differentiation, express negligible amounts of MPO mRNA, they have abundant MPO proteins (Yamada and Kurahashi, 1984; Sagoh and Yamada, 1988; Tobler et al., 1988). Neutrophils are the main source of MPO (Schultz and Kaminker, 1962), but although it was previously suggested that MPO is only produced by myeloid-lineage cells, Okada and collaborators identified MPO in peritoneal murine lymphocytes as well as in human lymphocytes from peripheral blood (de Araujo et al., 2013; Okada et al., 2016).

Results from the luminol experiments indicate that the PFAA and Cl-containing sub-mixtures induce a concentration-dependent increase in ROS production in human leucocytes. For neutrophils and lymphocytes, the increase was only significant at levels exceeding average exposure levels in the Scandinavian population. The Br mixture had little impact alone, but contributed to ROS production in combined mixtures. Indeed, lymphocytes exposed to the total mixture (PFAA + Cl + Br) produced more ROS than DMSO control even at the lowest concentration applied, corresponding to levels of these mixtures documented in blood samples from Scandinavians. Monocytes exhibited a significant increase in ROS production for all mixtures, even at the lowest concentrations (Figs. 1–3).

In the DCF experiments, the same tendencies were found in neutrophils for the PFAA and Cl mixtures. However, the increase in ROS production induced by the PFAA and Cl mixtures alone did not reach statistical significance even at the highest concentrations tested (Fig. 4). We believe this to be a power issue, since fewer replications of the DCF experiments were performed. Another explanation could be that the two methods detect different ROS (Myhre et al., 2003). Notably, the Br mixture alone seemed to have a concentration-dependent negative effect on ROS production in the DCF assay, whereas no significant effect of Br mixture alone could be detected for neutrophils in the luminol assay. This does not rule out that a true negative effect was present also in the luminol assay, although it may have been too small to detect.

The failure to detect increased ROS applying the probes luminol and DCF in neutrophils by Reistad and Mariussen (2005) mentioned above is interesting and may be a potential explanation also for the lack of ROS detection for the brominated mixture in the present study. However; as the concentrations of individual brominated mixture components in our study are mostly 1000 times lower than concentrations in the Reistad and Mariussen (2005) study (see Supplementary Table S1) even at our current highest tested concentration of 1000× human blood levels (range: 1–65 nM), it is unlikely that an effect would have been observed for the brominated mixture also with the application of a different assay such as the lucigenin assay. We could not find published studies on ROS production in blood cells for all the single components of the mixtures. However, across all halogenated groups, concentrations of individual compounds in our mixtures (Supplementary Table S1) were far lower than concentrations of single compounds inducing effects on ROS production in previously published studies. In comparison to the above-mentioned studies on single compounds, the range for compounds at 1× human blood levels where effects were currently observed in lymphocytes and monocytes were 0.018–1.1 nM for the chlorinated, 0.001–0.065 nM for the brominated and 0.28–16.4 nM for the perfluorinated compounds. In neutrophils significant ROS production was only observed from 100× the average blood levels calculated for the Scandinavian population (range: 1.8–109 nM for chlorinated, 0.1–6.5 nM for brominated and 28–1637 nM for perfluorinated compounds). One should bear in mind however, that blood levels for the various compounds may vary with geographical location and certain populations with a diet based on fish and game, people living close to POP-contaminated areas or occupationally exposed workers may exhibit higher body burdens of POPs.

We found slight synergy between Br and Cl mixture components in the luminol-granulocyte model, between PFAA and Br in the luminol-lymphocyte model (Table 2), as well as between PFAA/Br and PFAA/Cl in the DCF-granulocyte model (Table 4). In monocytes, however, all interactions terms were negative – mixture combinations yielded less ROS production than the sum of expected effect of each mixture alone (Table 2). Nevertheless, the combined effect of the different halogenated groups in the POP mixtures were mostly additive. Recent reviews concluded that synergisms or antagonisms are relatively rare and support the use of dose addition as the default concept for anticipating the combined effects of chemicals unless there is specific evidence that interactions might be relevant (Martin et al., 2020). In a recent study on the same POP mixture, additive responses were generally observed on different developmental neurotoxicity endpoints, however a potentiated effect in particular by the combination of PFAA + Br and Br + Cl mixtures were in fact observed for the end-points synaptogenesis (number of synapses) and neurite outgrowth (neurite length) (Davidsen et al., 2021). This is the same tendency as we observed in the luminol-granulocyte model, the luminol-lymphocyte model and partly the DCF-granulocyte model. Although the present paper was not focused on identifying active compounds within the mixtures, this represent interesting future studies, which could be conducted using single compounds.

It should be noted that cells in the present study were exposed *in vitro*, and also that the halogenated compounds of the mixtures in blood tend to accumulate in lipids or bind to plasma proteins, so the fraction of

compounds actually available for interaction with cells is uncertain. Despite this, the fact that these mixtures induced ROS production at levels found in human blood, and also that compounds from different halogenated groups seemed to act additively, is concerning. Taken into consideration the fact that we find a large number of anthropogenic chemicals in human blood, it is not unlikely that other compounds may potentially also add to POP-induced ROS production in blood cells.

4.3. Model considerations:

For the DCF assay, we did not have enough data to fit a linear mixed model. We applied a sandwich estimator to safeguard against type one errors in case the covariance structure was misspecified. However, with few groups, the GEE procedure may produce overly narrow confidence intervals. Nevertheless, since findings from the DCF assay correspond closely to those from the luminol assay, we do not believe our findings are spurious.

5. Conclusion

Using a linear mixed model, we show that a human relevant mixture and sub-mixtures of halogenated POPs induce concentration-dependent ROS production in three different types of human leucocytes *in vitro*. Importantly, increased ROS production was observed at concentrations corresponding to levels reported in human blood, underscoring that these effects may potentially be relevant also for real life exposure scenarios. Although some interactions were detected, our results support that halogenated subgroups of POPs mainly act additively. Furthermore, the POP-mixture-induced ROS responses in neutrophils appeared to involve activation of β2ARs. Even though more in-depth studies would be required to elucidate the role of β2ARs in these responses, our findings extend previous studies on PAH-induced β2AR impairment, suggesting that a broad range of environmental pollutants may interfere with adrenergic pathways. Given the central role of βARs in regulating cardiopulmonary function, immune responses and homeostasis, we believe that the potential impact of pollutants on the adrenergic system requires further attention.

CRediT authorship contribution statement

Hanne Friis Berntsen: Conceptualization, Methodology, Formal analysis, Investigation, Writing – original draft, Writing – review & editing, Visualization. **Johanna Bodin:** Conceptualization, Methodology, Formal analysis, Investigation, Writing – original draft, Writing – review & editing, Visualization. **Johan Øvrevik:** Conceptualization, Methodology, Formal analysis, Investigation, Writing – original draft, Writing – review & editing, Visualization. **Christopher Friis Berntsen:** Formal analysis, Writing – original draft, Writing – review & editing, Visualization. **Gunn Østby:** Investigation, Writing – review & editing. **Bendik C. Brinchmann:** Investigation, Writing – review & editing. **Erik Ropstad:** Conceptualization, Writing – original draft, Writing – review & editing, Funding acquisition. **Oddvar Myhre:** Conceptualization, Methodology, Investigation, Writing – original draft, Writing – review & editing, Visualization.

Declaration of Competing Interest

The authors declare that they have no known competing financial interests or personal relationships that could have appeared to influence the work reported in this paper.

Acknowledgement

Appendix A. Supplementary material

Supplementary data to this article can be found online at https://doi.org/10.1016/j.envint.2021.106900.

References

Aam, B.B., Fonnum, F., 2006. (+/-)-2-Chloropropionic acid elevates reactive oxygen species formation in human neutrophil granulocytes. Toxicology 228 (2–3), 124–134.

Abraham, K., Mielke, H., Fromme, H., Völkel, W., Menzel, J., Peiser, M., Zepp, F., Willich, S.N., Weikert, C., 2020. Internal exposure to perfluoroalkyl substances (PFASs) and biological markers in 101 healthy 1-year-old children: associations between levels of perfluorooctanoic acid (PFOA) and vaccine response. Arch. Toxicol. 94 (6), 2131–2147.

Arkoosh, M.R., Clemons, E., Myers, M., Casillas, E., 1994. Suppression of B-Cell Mediated Immunity in Juvenile Chinook Salmon (Oncorhynchus Tshawytscha) After Exposure To Either A Polycyclic Aromatic Hydrocan or To Polychlorinated Biphenyls. Immunopharmacol. Immunotoxicol. 16 (2), 293–314.

Audet, M., Bouvier, M., 2008. Insights into signaling from the beta2-adrenergic receptor structure. Nat. Chem. Biol. 4 (7), 397–403.

Barnett, C.C., Moore, E.E., Partrick, D.A., Silliman, C.C., 1997. β-Adrenergic Stimulation Down-Regulates Neutrophil Priming for Superoxide Generation, but Not Elastase Release. J. Surg. Res. 70 (2), 166–170.

Bates, D., Mächler, M., Bolker, B., Walker, S., 2014. Fitting linear mixed-effects models using lme4. arXiv preprint arXiv:1406.5823.

Bernstein, D., Fajardo, G., Zhao, M., 2011. The role of β-adrenergic receptors in heart failure: differential regulation of cardiotoxicity and cardioprotection. Prog. Pediatr. Cardiol. 31 (1), 35–38.

Berntsen, H.F., Berg, V., Thomsen, C., Ropstad, E., Zimmer, K.E., 2017. The design of an environmentally relevant mixture of persistent organic pollutants for use in in vivo and in vitro studies. J. Toxicol. Environ. Health A 80 (16–18), 1002–1016.

Berntsen, H.F., Bogen, I.L., Wigestrand, M.B., Fonnum, F., Walaas, S.I., Moldes-Anaya, A., 2017. The fungal neurotoxin penitrem A induces the production of reactive oxygen species in human neutrophils at submicromolar concentrations. Toxicology 392, 64–70.

Berntsen, H.F., Bolling, A.K., Bjorklund, C.G., Zimmer, K., Ropstad, E., Zienolddiny, S., Becher, R., Holme, J.A., Dirven, H., Nygaard, U.C., Bodin, J., 2018. Decreased macrophage phagocytic function due to xenobiotic exposures in vitro, difference in sensitivity between various macrophage models. Food Chem. Toxicol. 112, 86–96.

Berntsen, H.F., Duale, N., Bjørklund, C.G., Rangel-Huerta, O.D., Dyrberg, K., Hofer, T., Rakkestad, K.E., Østby, G., Halsne, R., Boge, G., Paulsen, R.E., Myhre, O., Ropstad, E., 2021. Effects of a human-based mixture of persistent organic pollutants on the in vivo exposed cerebellum and cerebellar neuronal cultures exposed in vitro. Environ. Int. 146, 106240.

Berntsen, H.F., Fonnum, F., Walaas, S.I., Bogen, I.L., 2016. Low-Chlorinated Non-Dioxin-like Polychlorinated Biphenyls Present in Blood and Breast Milk Induce Higher Levels of Reactive Oxygen Species in Neutrophil Granulocytes than High-Chlorinated Congeners. Basic Clin. Pharmacol. Toxicol. 119 (6), 588–597.

Boyum, A., Lovhaug, D., Tresland, L., Nordlie, E.M., 1991. Separation of leucocytes: improved cell purity by fine adjustments of gradient medium density and osmolality. Scand. J. Immunol. 34 (6), 697–712.

Buck, A., Sanchez Klose, F.P., Venkatakrishnan, V., Khamzeh, A., Dahlgren, C., Christenson, K., Bylund, J., 2019. DPI Selectively Inhibits Intracellular NADPH Oxidase Activity in Human Neutrophils. Immunohorizons 3 (10), 488–497.

Cazzola, M., Calzetta, L., Matera, M.G., 2011. β(2) -adrenoceptor agonists: current and future direction. Br. J. Pharmacol. 163 (1), 4–17.

Chu, S., Zhang, H., Maher, C., McDonald, J.D., Zhang, X., Ho, S.M., Yan, B., Chillrud, S., Perera, F., Factor, P., Miller, R.L., 2013. Prenatal and postnatal polycyclic aromatic hydrocarbon exposure, airway hyperreactivity, and Beta-2 adrenergic receptor function in sensitized mouse offspring. J. Toxicol. 2013, 603581.

Corsini, E., Sokooti, M., Galli, C.L., Moretto, A., Colosio, C., 2013. Pesticide induced immunotoxicity in humans: a comprehensive review of the existing evidence. Toxicology 307, 123–135.

Dahlgren, C., Karlsson, A., 1999. Respiratory burst in human neutrophils. J. Immunol. Methods 232 (1–2), 3–14.

Davidsen, N., Lauvås, A.J., Myhre, O., Ropstad, E., Carpi, D., Gyves, E.M., Berntsen, H.F., Dirven, H., Paulsen, R.E., Bal-Price, A., Pistollato, F., 2021. Exposure to human relevant mixtures of halogenated persistent organic pollutants (POPs) alters neurodevelopmental processes in human neural stem cells undergoing differentiation. Reprod Toxicol. 100, 17–34.

de Araujo, T.H., Okada, S.S., Ghosn, E.E.B., Taniwaki, N.N., Rodrigues, M.R., de Almeida, S.R., Mortara, R.A., Russo, M., Campa, A., Albuquerque, R.C., 2013. Intracellular localization of myeloperoxidase in murine peritoneal B-lymphocytes and macrophages. Cell. Immunol. 281 (1), 27–30.

Deupi, X., Kobilka, B.K., 2010. Energy landscapes as a tool to integrate GPCR structure, dynamics, and function. Physiology (Bethesda) 25 (5), 293–303.

Di Lisa, F., Kaludercic, N., Paolocci, N., 2011. β₂-Adrenoceptors, NADPH oxidase, ROS and p38 MAPK: another 'radical' road to heart failure? Br. J. Pharmacol. 162 (5), 1009–1011.

Dowle, M., Srinivasan, A., 2019. data. table: Extension ofdata. frame. R package version 1.12. 2. ed.

Drake, M.T., Violin, J.D., Whalen, E.J., Wisler, J.W., Shenoy, S.K., Lefkowitz, R.J., 2008. beta-arrestin-biased agonism at the beta2-adrenergic receptor. J. Biol. Chem. 283 (9), 5669–5676.

EFSA, 2020. Risk to human health related to the presence of perfluoroalkyl substances in food. EFSA J 18(9), e06223-e06223.

Ermler, S., Scholze, M., Kortenkamp, A., 2013. Seven benzimidazole pesticides combined at sub-threshold levels induce micronuclei in vitro. Mutagenesis 28 (4), 417–426.

Evans, B.A., Sato, M., Sarwar, M., Hutchinson, D.S., Summers, R.J., 2010. Ligand-directed signalling at beta-adrenoceptors. Br. J. Pharmacol. 159 (5), 1022–1038.

Factor, P., Akhmedov, A.T., McDonald, J.D., Qu, A., Wu, J., Jiang, H., Dasgupta, T., Panettieri Jr., R.A., Perera, F., Miller, R.L., 2011. Polycyclic aromatic hydrocarbons impair function of β2-adrenergic receptors in airway epithelial and smooth muscle cells. Am. J. Respir. Cell Mol. Biol. 45 (5), 1045–1049.

Freberg, B.I., Haug, L.S., Olsen, R., Daae, H.L., Hersson, M., Thomsen, C., Thorud, S., Becher, G., Molander, P., Ellingsen, D.G., 2010. Occupational Exposure to Airborne Perfluorinated Compounds during Professional Ski Waxing. Environ. Sci. Technol. 44 (19), 7723–7728.

Froot, K.A., 1989. Consistent covariance matrix estimation with cross-sectional dependence and heteroskedasticity in financial data. J. Financ. Quantit. Anal. 333–355.

Futosi, K., Fodor, S., Mócsai, A., 2013. Neutrophil cell surface receptors and their intracellular signal transduction pathways. Int. Immunopharmacol. 17 (3), 638–650.

Gimenez, L.E., Baameur, F., Vayttaden, S.J., Clark, R.B., 2015. Salmeterol Efficacy and Bias in the Activation and Kinase-Mediated Desensitization of β2-Adrenergic Receptors. Mol. Pharmacol. 87 (6), 954–964.

Grandjean, P., Andersen, E.W., Budtz-Jørgensen, E., Nielsen, F., Mølbak, K., Weihe, P., Heilmann, C., 2012. Serum vaccine antibody concentrations in children exposed to perfluorinated compounds. JAMA 307 (4), 391–397.

Grandjean, P., Heilmann, C., Weihe, P., Nielsen, F., Mogensen, U.B., Budtz-Jørgensen, E., 2017a. Serum Vaccine Antibody Concentrations in Adolescents Exposed to Perfluorinated Compounds. Environ. Health Perspect. 125(7), 077018-077018.

Grandjean, P., Heilmann, C., Weihe, P., Nielsen, F., Mogensen, U.B., Timmermann, A., Budtz-Jørgensen, E., 2017. Estimated exposures to perfluorinated compounds in infancy predict attenuated vaccine antibody concentrations at age 5-years. J. Immunotoxicol. 14 (1), 188–195.

Gullberg, U., Bengtsson, N., Bülow, E., Garwicz, D., Lindmark, A., Olsson, I., 1999. Processing and targeting of granule proteins in human neutrophils. J. Immunol. Methods 232 (1), 201–210.

Halekoh, U., Højsgaard, S., Yan, J., 2006. The R package geepack for generalized estimating equations. J. Statist. Software 15 (2), 1–11.

Harrison, J.E., Schultz, J., 1976. Studies on the chlorinating activity of myeloperoxidase. J. Biol. Chem. 251 (5), 1371–1374.

Heilmann, C., Grandjean, P., Weihe, P., Nielsen, F., Budtz-Jørgensen, E., 2006. Reduced antibody responses to vaccinations in children exposed to polychlorinated biphenyls. PLoS Med. 3(8), e311-e311.

Hothorn, T., Bretz, F., Westfall, P., 2008. Simultaneous inference in general parametric models. Biom. J. 50 (3), 346–363.

Jackson, S.H., Devadas, S., Kwon, J., Pinto, L.A., Williams, M.S., 2004. T cells express a phagocyte-type NADPH oxidase that is activated after T cell receptor stimulation. Nat. Immunol. 5 (8), 818–827.

Jancinová, V., Drábiková, K., Nosál, R., Racková, L., Májeková, M., Holománová, D., 2006. The combined luminol/isoluminol chemiluminescence method for differentiating between extracellular and intracellular oxidant production by neutrophils. Redox Rep. 11 (3), 110–116.

Jones, P.D., Hu, W., De Coen, W., Newsted, J.L., Giesy, J.P., 2003. Binding of perfluorinated fatty acids to serum proteins. Environ. Toxicol. Chem. 22 (11), 2639–2649.

Kalyanaraman, B., Darley-Usmar, V., Davies, K.J., Dennery, P.A., Forman, H.J., Grisham, M.B., Mann, G.E., Moore, K., Roberts, L.J.2nd., Ischiropoulos, H., 2012. Measuring reactive oxygen and nitrogen species with fluorescent probes: challenges and limitations. Free Radic. Biol. Med. 52(1), 1–6.

Karlsson, M., Kurz, T., Brunk, U.T., Nilsson, S.E., Frennesson, C.I., 2010. What does the commonly used DCF test for oxidative stress really show? Biochem J. 428 (2), 183–190.

Karrman, A., van Bavel, B., Jarnberg, U., Hardell, L., Lindstrom, G., 2006. Perfluorinated chemicals in relation to other persistent organic pollutants in human blood. Chemosphere 64 (9), 1582–1591.

Khan, P., Idrees, D., Moxley, M.A., Corbett, J.A., Ahmad, F., von Figura, G., Sly, W.S., Waheed, A., Hassan, M.I., 2014. Luminol-based chemiluminescent signals: clinical and non-clinical application and future uses. Appl Biochem Biotechnol. 173 (2), 333–355.

Kizaki, T., Izawa, T., Sakurai, T., Haga, S., Taniguchi, N., Tajiri, H., Watanabe, K., Day, N. K., Toba, K., Ohno, H., 2008. Beta2-adrenergic receptor regulates Toll-like receptor-4-induced nuclear factor-kappaB activation through beta-arrestin 2. Immunology. 124 (3), 348–356.

Kortenkamp, A., Backhaus, T., Faust, M., 2009. State of the Art Report on Mixture Toxicity. Final Report. Executive Summary. The School of Pharmacy University of London (ULSOP).

Kuznetsova, A., Brockhoff, P.B., Christensen, R.H.B., 2017. lmerTest Package: Tests in Linear Mixed Effects Models. J. Statist. Software 1 (13), 2017.

Lau, C., 2012. Perfluorinated compounds, in: Luch, A. (Ed.) Molecular, clinical and environmental toxicology. Volume 3: Environmental Toxicology. Springer Basel, Basel, pp. 47-86.

Le Ferrec, E., Øvrevik, J., 2018. G-protein coupled receptors (GPCR) and environmental exposure. Consequences for cell metabolism using the β-adrenoceptors as example. Curr. Opin. Toxicol. 8, 14–19.

LeBel, C.P., Ischiropoulos, H., Bondy, S.C., 1992. Evaluation of the probe 2′,7′-dichlorofluorescin as an indicator of reactive oxygen species formation and oxidative stress. Chem. Res. Toxicol. 5 (2), 227–231.

Leijs, M.M., Koppe, J.G., Olie, K., Aalderen, W.M.C.v., Voogt, P.d., Tusscher, G.W.t., 2009. Effects of Dioxins, PCBs, and PBDEs on Immunology and Hematology in Adolescents. Environ. Sci. Technol. 43(20), 7946-7951.

Lucas, K., Maes, M., 2013. Role of the Toll Like receptor (TLR) radical cycle in chronic inflammation: possible treatments targeting the TLR4 pathway. Mol Neurobiol. 48 (1), 190–204.

Malech, H.L., Deleo, F.R., Quinn, M.T., 2014. The role of neutrophils in the immune system: an overview. Methods in molecular biology (Clifton, N.J.) 1124, 3-10.

Mangum, L.C., Borazjani, A., Stokes, J.V., Matthews, A.T., Lee, J.H., Chambers, J.E., Ross, M.K., 2015. Organochlorine insecticides induce NADPH oxidase-dependent reactive oxygen species in human monocytic cells via phospholipase A2/arachidonic acid. Chem. Res. Toxicol. 28 (4), 570–584.

Martin, O., Scholze, M., Ermler, S., McPhie, J., Bopp, S.K., Kienzler, A., Parissis, N., Kortenkamp, A., 2020. Ten years of research on synergisms and antagonisms in chemical mixtures: A systematic review and quantitative reappraisal of mixture studies. Environ. Int. 146, 106206.

Mayati, A., Le Ferrec, E., Holme, J.A., Fardel, O., Lagadic-Gossmann, D., Øvrevik, J., 2014. Calcium signaling and β2-adrenergic receptors regulate 1-nitropyrene induced CXCL8 responses in BEAS-2B cells. Toxicol. In Vitro 28 (6), 1153–1157.

Mayati, A., Levoin, N., Paris, H., N'Diaye, M., Courtois, A., Uriac, P., Lagadic-Gossmann, D., Fardel, O., Le Ferrec, E., 2012. Induction of intracellular calcium concentration by environmental benzo(a)pyrene involves a β2-adrenergic receptor/adenylyl cyclase/Epac-1/inositol 1,4,5-trisphosphate pathway in endothelial cells. J. Biol. Chem. 287 (6), 4041–4052.

Mayati, A., Podechard, N., Rineau, M., Sparfel, L., Lagadic-Gossmann, D., Fardel, O., Le Ferrec, E., 2017. Benzo(a)pyrene triggers desensitization of β2-adrenergic pathway. Sci. Rep. 7 (1), 3262.

Myhre, O., Andersen, J.M., Aarnes, H., Fonnum, F., 2003. Evaluation of the probes 2′,7′-dichlorofluorescin diacetate, luminol, and lucigenin as indicators of reactive species formation. Biochem. Pharmacol. 65 (10), 1575–1582.

Myhre, O., Mariussen, E., Reistad, T., Voie, O.A., Aarnes, H., Fonnum, F., 2009. Effects of polychlorinated biphenyls on the neutrophil NADPH oxidase system. Toxicol. Lett. 187 (3), 144–148.

Myhre, O., Vestad, T.A., Sagstuen, E., Aarnes, H., Fonnum, F., 2000. The effects of aliphatic (n-nonane), naphtenic (1,2, 4-trimethylcyclohexane), and aromatic (1,2,4-trimethylbenzene) hydrocarbons on respiratory burst in human neutrophil granulocytes. Toxicol. Appl. Pharmacol. 167 (3), 222–230.

Nakanishi, Y., Shigematsu, N., Kurita, Y., Matsuba, K., Kanegae, H., Ishimaru, S., Kawazoe, Y., 1985. Respiratory involvement and immune status in yusho patients. Environ. Health Perspect. 59, 31–36.

Nilsson, H., Karrman, A., Westberg, H., Rotander, A., van Bavel, B., Lindstrom, G., 2010. A time trend study of significantly elevated perfluorocarboxylate levels in humans after using fluorinated ski wax. Environ. Sci. Technol. 44 (6), 2150–2155.

Okada, S.S., de Oliveira, E.M., de Araújo, T.H., Rodrigues, M.R., Albuquerque, R.C., Mortara, R.A., Taniwaki, N.N., Nakaya, H.I., Campa, A., Moreno, A.C.R., 2016. Myeloperoxidase in human peripheral blood lymphocytes: Production and subcellular localization. Cell. Immunol. 300, 18–25.

Opdahl, H., Benestad, H.B., Nicolaysen, G., 1993. Effect of beta-adrenergic agents on human neutrophil granulocyte activation with N-formyl-methionyl-leucyl-phenylalanine and phorbol myristate acetate. Pharmacol. Toxicol. 72 (4–5), 221–228.

Panday, A., Sahoo, M.K., Osorio, D., Batra, S., 2015. NADPH oxidases: an overview from structure to innate immunity-associated pathologies. Cell. Mol. Immunol. 12 (1), 5–23.

Pistollato, F., de Gyves, E.M., Carpi, D., Bopp, S.K., Nunes, C., Worth, A., Bal-Price, A., 2020. Assessment of developmental neurotoxicity induced by chemical mixtures using an adverse outcome pathway concept. Environ. Health 19 (1), 23.

R Core Team, 2019. R: A Language and Environment for Statistical Computing; R Foundation for Statistical Computing: Vienna, Austria, 2019.© 2020 by the authors. Licensee MDPI, Basel, Switzerland. This article is an open access article distributed under the terms and conditions of the Creative Commons Attribution (CC BY) license (http://creativecommons. org/licenses/by/4.0/).

Rambacher, K.M., Moniri, N.H., 2020. The β2-adrenergic receptor-ROS signaling axis: An overlooked component of β2AR function? Biochem. Pharmacol. 171, 113690.

Reistad, T., Mariussen, E., 2005. A commercial mixture of the brominated flame retardant pentabrominated diphenyl ether (DE-71) induces respiratory burst in human neutrophil granulocytes in vitro. Toxicol. Sci. 87 (1), 57–65.

Repnik, U., Knezevic, M., Jeras, M., 2003. Simple and cost-effective isolation of monocytes from buffy coats. J. Immunol. Methods 278 (1–2), 283–292.

Robinson, D., Hayes, A., Couch, S., 2019. Broom: Convert statistical objects into tidy tibbles.

Rosenbaum, D.M., Rasmussen, S.G.F., Kobilka, B.K., 2009. The structure and function of G-protein-coupled receptors. Nature 459 (7245), 356–363.

Sagoh, T., Yamada, M., 1988. Transcriptional regulation of myeloperoxidase gene expression in myeloid leukemia HL-60 cells during differentiation into granulocytes and macrophages. Arch. Biochem. Biophys. 262 (2), 599–604.

Salon, J.A., Lodowski, D.T., Palczewski, K., 2011. The Significance of G Protein-Coupled Receptor Crystallography for Drug Discovery. Pharmacol. Rev. 63 (4), 901.

Scanzano, A., Cosentino, M., 2015. Adrenergic regulation of innate immunity: a review. Front. Pharmacol. 6, 171-171.

Schultz, J., Kaminker, K., 1962. Myeloperoxidase of the leucocyte of normal human blood. I. Content and localization. Arch. Biochem. Biophys. 96, 465–467.

Secretariat of the Stockholm Convention, 2019a. What are POPs? http://chm.pops. int/TheConvention/ThePOPs/tabid/673/Default.aspx. (Accessed 20.12 2020).

Secretariat of the Stockholm Convention, 2019b. Chemicals proposed for listing under the Convention. http://chm.pops.int/TheConvention/ThePOPs/ChemicalsPropo sedforListing/tabid/2510/Default.aspx. (Accessed Desember 5th 2020).

Seifert, R., Schultz, G., 1991. The superoxide-forming NADPH oxidase of phagocytes. An enzyme system regulated by multiple mechanisms. Rev. Physiol. Biochem. Pharmacol. 117, 1–338.

Selvatici, R., Falzarano, S., Mollica, A., Spisani, S., 2006. Signal transduction pathways triggered by selective formylpeptide analogues in human neutrophils. Eur. J. Pharmacol. 534 (1–3), 1–11.

Tampo, Y., Kotamraju, S., Chitambar, C.R., Kalivendi, S.V., Keszler, A., Joseph, J., Kalyanaraman, B., 2003. Oxidative stress-induced iron signaling is responsible for peroxide-dependent oxidation of dichlorodihydrofluorescein in endothelial cells: role of transferrin receptor-dependent iron uptake in apoptosis. Circ. Res. 92 (1), 56–63.

Tobler, A., Miller, C.W., Johnson, K.R., Selsted, M.E., Rovera, G., Koeffler, H.P., 1988. Regulation of gene expression of myeloperoxidase during myeloid differentiation. J. Cell. Physiol. 136 (2), 215–225.

Voie, O.A., Tysklind, M., Andersson, P.L., Fonnum, F., 2000. Activation of respiratory burst in human granulocytes by polychlorinated biphenyls: A structure-activity study. Toxicol. Appl. Pharmacol. 167 (2), 118–124.

Voie, Ø.A., Wiik, P., Fonnum, F., 1998. Ortho-substituted polychlorinated biphenyls activate respiratory burst measured as luminol-amplified chemoluminescence in human granulocytes. Toxicol. Appl. Pharmacol. 150 (2), 369–375.

Wenzel-Seifert, K., Ervens, J., Seifert, R., 1991. Differential inhibition and potentiation by cell-permeant analogues of cyclic AMP and cyclic GMP and NO-containing compounds of exocytosis in human neutrophils. Naunyn Schmiedebergs Arch. Pharmacol. 344 (4), 396–402.

Wickham, H., 2016. ggplot2: elegant graphics for data analysis. springer.

Wickham, H., François, R., 2019. dplyr: A Grammar of Data Manipulation.

Williams, R.L., 2000. A note on robust variance estimation for cluster-correlated data. Biometrics 56 (2), 645–646.

Wrona, M., Wardman, P., 2006. Properties of the radical intermediate obtained on oxidation of 2',7'-dichlorodihydrofluorescein, a probe for oxidative stress. Free Radic Biol Med. 41 (4), 657–667.

Xu, Q., Dalic, A., Fang, L., Kiriazis, H., Ritchie, R.H., Sim, K., Gao, X.M., Drummond, G., Sarwar, M., Zhang, Y.Y., Dart, A.M., Du, X.J., 2011. Myocardial oxidative stress contributes to transgenic β₂-adrenoceptor activation-induced cardiomyopathy and heart failure. Br. J. Pharmacol. 162 (5), 1012–1028.

Yamada, M., Kurahashi, K., 1984. Regulation of myeloperoxidase gene expression during differentiation of human myeloid leukemia HL-60 cells. J. Biol. Chem. 259 (5), 3021–3025.

Yan, J., 2002. Geepack: yet another package for generalized estimating equations. R-news 2 (3), 12–14.

Yan, J., Fine, J., 2004. Estimating equations for association structures. Stat. Med. 23 (6), 859–874.

Zarei, M.H., Hosseini Shirazi, S.F., Aghvami, M., Pourahmad, J., 2018. Perfluorooctanesulfonate (PFOS) Induces Apoptosis Signaling and Proteolysis in Human Lymphocytes through ROS Mediated Mitochondrial Dysfunction and Lysosomal Membrane Labialization. Iran J Pharm Res 17 (3), 995–1007.

Zeng, W., Wang, Y., Liu, Z., Khanniche, A., Hu, Q., Feng, Y., Ye, W., Yang, J., Wang, S., Zhou, L., Shen, H., Wang, Y., 2014. Long-term exposure to decabrominated diphenyl ether impairs CD8 T-cell function in adult mice. Cell. Mol. Immunol. 11 (4), 367–376.

Zhang, Y.H., Wang, J., Dong, G.H., Liu, M.M., Wang, D., Zheng, L., Jin, Y.H., 2013. Mechanism of perfluorooctanesulfonate (PFOS)-induced apoptosis in the immunocyte. J. Immunotoxicol. 10 (1), 49–58.